UC Riverside
UC Riverside Previously Published Works

Title

Groundwater recharge from drywells under constant head conditions

Permalink

https://escholarship.org/uc/item/5c70r44z

Authors

Sasidharan, Salini
Bradford, Scott A
Šimůnek, Jiří
et al.

Publication Date

2020-04-01

DOI

10.1016/j.jhydrol.2020.124569

Peer reviewed

Groundwater Recharge from Drywells Under Constant Head Conditions

Salini Sasidharan[1,2,*], **Scott A. Bradford**[2], **Jiří Šimůnek**[1], **Stephen R. Kraemer**[3]

[1]Department of Environmental Sciences, University of California Riverside, Riverside, CA 92521, USA

[2]United States Department of Agriculture, Agricultural Research Service, U. S. Salinity Laboratory, Riverside, CA 92507, USA

[3]U.S. Environmental Protection Agency, Office of Research and Development, Los Angeles, CA 90017

Abstract

Drywells are widely used as managed aquifer recharge devices to capture stormwater runoff and recharge groundwater, but little research has examined the role of subsurface heterogeneity in hydraulic properties on drywell recharge efficiency. Numerical experiments were therefore conducted on a 2D-axisymmetric domain using the HYDRUS (2D/3D) software to systematically study the influence of various homogenous soil types and subsurface heterogeneity on recharge from drywells under constant head conditions. The mean cumulative infiltration (μI) and recharge (μR) volumes increased with an increase in the saturated hydraulic conductivity (K_s) for various homogeneous soils. Subsurface heterogeneity was described by generating ten stochastic realizations of soil hydraulic properties with selected standard deviation (σ), and horizontal (X) and vertical (Z) correlation lengths. After 365 days, values of μI, μR, and the radius of the recharge area increased with σ and X but decreased with Z. The value of μR was always smaller for a homogeneous than a heterogeneous domain. This indicates that recharge for a heterogeneous profile cannot be estimated with an equivalent homogeneous profile. The value of μR was always smaller than μI and correlations were highly non-linear due to vadose zone storage. Knowledge of only infiltration volume can, therefore, lead to misinterpretation of recharge efficiency, especially

[*]Corresponding Author: Salini Sasidharan, USDA, ARS, Salinity Laboratory, Riverside, CA 92507, United States, Phone: +951-369-4823, salinis@ucr.edu.

Author Contribution

1.   **Salini Sasidharan:** Investigation, Methodology, Software, Formal Analysis, Validation, Data Curation, Synthesis of Result, Writing - Original Draft, Visualization

2.   **Scott A. Bradford:** Conceptualization of the Project, Software, Resources, Synthesis of Result, Writing - Review & Editing, Supervision, Project Administration

3.   **Jiří Šimůnek:** Conceptualization of the Project, Software, Resources, Synthesis of Result, Writing - Review & Editing, Supervision, Project Administration

4.   **Stephen R. Kraemer:** Writing - Review & Editing, Project Administration, Funding Acquisition

8.·SUPPLEMENTARY MATERIAL
Figures S1, S2, S3, S4, S5, S6, S7, and S8 can be found in the Supporting Information file.

at earlier times. The arrival time of the wetting front at the bottom boundary (60 m) ranged from 21-317 days, with earlier times occurring for increasing σ and Z. The corresponding first arrival location can be 0.1-44 m away from the bottom releasing point of a drywell in the horizontal direction, with greater distances occurring for increasing σ and X. This knowledge is important to accurately assess drywell recharged performance, water quantity, and water quality.

GRAPHICAL ABSTRACT

10.
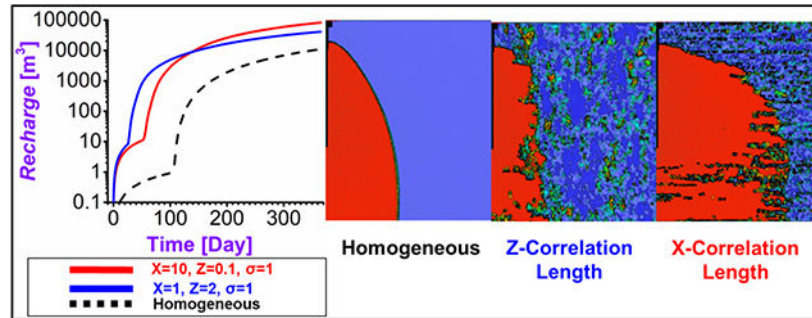
Keywords

Drywell; Infiltration; Recharge; Arrival time; Arrival location; HYDRUS (2D/3D)

1. INTRODUCTION

The World Economic Forum lists freshwater scarcity as the largest global risk to the sustainable development of human society due to the increasing demand of the world population and expansion of irrigated agriculture (Ercin and Hoekstra, 2014; Mekonnen and Hoekstra, 2016; Vorosmarty et al., 2000). Spatial and temporal variations in water demand lead to water scarcity in several parts of the world during specific times of the year (Mekonnen and Hoekstra, 2016; Postel et al., 1996; Savenije, 2000). Water resources can be divided into renewable (e.g., surface water and groundwater) and non-renewable (deep aquifers, which do not have a significant replenishment rate on the human time scale) (Mancosu et al., 2015). Groundwater is a vital source of freshwater, (Zektser and Lorne, 2004), however, overexploitation of groundwater resources has resulted in groundwater depletion, increased pollution, land subsidence, soil salinization, and seawater intrusion in parts of the world (Feng et al., 2013). Urban development with impermeable and paved surfaces leads to reduced infiltration of runoff water and extreme flooding events, but also offers opportunities to capture and store excess runoff and recharge groundwater. Increased flooding from climate extremes also provides opportunities for collecting, storing, and injecting stormwater into an aquifer for use during droughts (Scanlon et al., 2016).

Sustainable utilization of water resources can be achieved by reducing the demand for groundwater through increased water use efficiency, conjunctive use of alternative water sources, or increasing recharge (Dillon et al. 2012). Stormwater capture, infiltration, and recharge technologies such as infiltration basins, vadose zone infiltration devices like

drywells (Edwards et al., 2016; Sasidharan et al., 2018a; Sasidharan et al., 2019), infiltration trenches, stormwater wells, and direct injection wells (Dillon, 2005; Gale, 2005; Richard and Peter, 2017) have been developed over the last 60 years. The main focuses of all these managed aquifer recharge strategies are to prevent flooding and surface and groundwater pollution, enhance drought resilience with short-term coping strategies and long-term adaptive capacity, and increase groundwater recharge (Dillon et al., 2019; Scanlon et al., 2016; Washington State Department of Ecology, 2006). A few major cities in California and Washington achieve nearly 70-100 percent of their groundwater recharge through stormwater drainage wells or drywell infiltration (Cadmus, 1999; EPA, 1999). Similarly, rapidly developing urban areas, in Arizona, Florida, and Texas, are planning to continue to build stormwater wells as a cost-effective way to manage runoff and to recharge groundwater (Cadmus, 1999; EPA, 1999).

Accurate estimation of groundwater recharge remains a challenge in the field of hydrology due to its nonlinear nature, which varies with space and time (Wang et al., 2016). Traditionally, both physical (water balance, Darcy flux, root-zone drainage) and chemical (tracers) approaches have been used to estimate recharge in arid and semi-arid areas (Allison et al., 1994). However, these techniques are expensive, not useful for short-term measurement, and exhibit large errors (Hendrickx and Walker, 2017; Huang et al., 2017). In addition, spatial variability in local topography, soil texture, and structure produce heterogeneity in groundwater recharge that requires a large number of sampling locations (Allison et al., 1994). Limited field measurements are increasingly used in combination with vadose zone numerical modeling as a time and cost-effective method to estimate groundwater recharge (Min et al., 2015; Ries et al., 2015; Small, 2005; Turkeltaub et al., 2015; Wang et al., 2016). However, most of these studies only considered root zone soil moisture, deep vadose zone soil water content, and matric pressure data to determine the average soil hydraulic parameters for the vadose zone to a maximum depth of 1-20 m. Furthermore, these investigations have shown large differences in groundwater recharge and simulated data due to uncertainty in model parameters.

Soil heterogeneity such as the presence of high and low permeable soil layers, their horizontal and vertical distribution, and connectivity significantly impacts water flow in the subsurface (Mantoglou and Gelhar, 1987; Schilling et al., 2017; Xie et al., 2014; Yeh et al., 1985a; Yeh et al., 1985b). Inadequate characterization of subsurface heterogeneity can lead to uncertainty in the prediction of water flow through the vadose zone, contaminant migration, and estimation of recharge. Deterministic and stochastic models can be used to study water flow in the vadose zone and groundwater recharge from a drywell. The Miller and Miller (1956) similitude scaling approach is a stochastic model that has been widely used to analyze flow and transport processes in heterogeneous unsaturated soil systems (Hammel and Roth, 1998; Roth, 1995; Roth and Hammel, 1996; Tseng and Jury, 1994; Vereecken et al., 2007). Our previous study investigated the influence of stochastic vadose zone heterogeneity on drywell infiltration behavior and determined the effective unsaturated soil hydraulic properties (Sasidharan et al., 2019). Most previous infiltration and recharge studies have looked at the long term steady-state conditions when infiltration (below the root zone) equals recharge (Gray and Norum, 1967; Mantoglou and Gelhar, 1987; Yeh et al., 1985a; Yeh et al., 1985b). However, the installation of a new drywell that receives episodic

water input will create transient conditions in the vadose zone that will change infiltration, recharge, and storage. In this case, infiltration will be greater than recharge until a new steady-state condition is achieved. Transient recharge behavior is important for drywells because during their typical operational lifespan (e.g., a decade) they may not ever achieve steady-state conditions. However, no literature has investigated the effect of subsurface heterogeneity on groundwater recharge from a drywell under constant head conditions, which is an upper bound (best-case scenario) for recharge and worst-case scenario for contaminant transport.

One of the major selling points for drywells compared to direct injection wells is the opportunity for vadose zone treatment of contaminants (Edwards et al., 2016). Current regulatory standards for drywells only require 1.5 to 13 m separation distance between the bottom of the drywell and the local groundwater table (City of Portland, 2008; City of Portland, 2015; EPA, 1999; Washington State Department of Ecology, 2006). However, many previous studies using microbial contaminants like viruses (Sasidharan et al., 2018b; Sasidharan et al., 2017a; Schijven and Hassanizadeh, 2000) and bacteria (Camesano and Logan, 1998; Johnson et al., 1995; Sasidharan et al., 2017b) demonstrated that microbial retention and inactivation is a function of the flow velocity and residence time. Soil profiles with high permeability or preferential flow paths (Arnaud et al., 2015; Bradford et al., 2017) can lead to the early arrival of pathogenic microbes at the water table. In addition, monitoring wells to characterize recharge water quality are usually installed within a few meters of a drywell (Hamad et al., 2016; Izuka, 2011). This implicitly assumes that the arrival of recharge water occurs directly below the bottom of the drywell. In many cases, drinking water supply wells have been contaminated or threatened by water infiltrated from drywells (i.e., stormwater drainage wells) (Haney et al., 1989). Varying degrees contamination of groundwater by stormwater drainage wells has been reported across the US (Cadmus, 1991; Cadmus, 1996; Cadmus, 1999; Haney et al., 1989; Michael, 1997; Orr, 1993; USEPA, 1997; Wilde, 1994). Therefore, an understanding of the influence of subsurface heterogeneity on the arrival time and location of recharge during the short-term operation of a drywell is essential when assessing water quality.

The objective of this study is to investigate the influence of subsurface heterogeneity on groundwater recharge from a drywell, especially the short-term condition when recharge does not yet equal infiltration. The HYDRUS (2D/3D) software was used to directly simulate cumulative infiltration and recharge volumes from a drywell for different homogenous and heterogeneous soils. Constant head conditions were considered in the drywell to facilitate the determination of subsurface soil properties on the upper limit for recharge (and contaminant transport) and the lower limit on arrival time. Subsurface heterogeneity was described in this model by generating stochastic realizations of soil hydraulic properties with selected standard deviation, and vertical and horizontal correlation lengths. The influence of stochastic subsurface heterogeneity parameters on cumulative infiltration (I) and recharge (R) volumes, the radius of recharge (r_x), early (EA_T) and late (LA_T) arrival times, and early (EA_P) and late (LA_P) arrival points were determined to understand the drywell infiltration and recharge behavior in the deep vadose zone (60 m).

2. MATERIALS AND METHODS

2.1 Mathematical Model

This research explores the role of subsurface heterogeneities on recharge from a drywell using numerical experiments. Input parameters, initial conditions, and boundary conditions that were employed in these numerical experiments were generally based on results from drywells located in Fort Irwin, CA that are discussed in the supporting information (SI). The HYDRUS (2D/3D) software package version 3 (Šejna et al., 2018; Šim nek et al., 2018; Šim nek et al., 2016) was used to simulate infiltration from the drywell, redistribution in the vadose zone, and recharge into the groundwater. HYDRUS (2D/3D) numerically solves the 2-dimensional axisymmetric form of Richards equation using the van Genuchten (1980) and Mualem (1976) unsaturated soil hydraulic functions. Unless otherwise stated default values of hydraulic parameters (e.g., the saturated soil hydraulic conductivity, K_s; the shape parameter in the soil water retention function, α; the residual soil water content, θ_r; the saturated soil water content, θ_s; the pore-size distribution parameter in the soil water retention function, n; and the tortuosity parameter in the hydraulic conductivity function, l) for various soil textural classes were taken from the HYDRUS (2D/3D) Soil Catalog (Carsel and Parrish, 1988; Šejna et al., 2014).

Fig. 1 shows a schematic of an example simulation flow domain, drywell geometry, initial condition, boundary conditions, and scale of the domain. The drywell geometry employed in this study was adapted from a MaxWell IV model (Torrents Resources, Phoenix, Arizona, USA) drywell (DW2) installed at the Fort Irwin study site (see section 1 in SI). The complex geometry of the drywell and the dynamics of the water flow from the drywell is described in detail by Sasidharan et al. (2018a). The drywell has a size of 36 m (Height, H) × 1.8 m (Width, W). A 60 m (H) × 50 m (W) simulation flow domain was chosen to best capture the infiltration radius of the drywell, to account for the drywell depth, and to accurately estimate the arrival time of the recharge water and rate (Fig. 1). The simulation domain was discretized using a two-dimensional triangular finite element mesh with the MESHGEN tool available within HYDRUS (2D/3D) (Šejna et al., 2014). The mesh was refined at the left part of the domain where infiltration from the drywell was simulated. To reduce the mass balance error, the finite element mesh was adjusted such that the size of elements was smaller (0.05-0.1 m) near the drywell and the grid size was gradually increased with radial distance from the drywell, with a maximum element size of 0.5-0.75 m. The quality of the finite element mesh was assessed by checking the mass balance error reported by HYDRUS (2D/3D) at the end of the simulation. Mass balance errors were always below 1%, and these values are generally considered acceptable (Brunetti et al., 2017).

A no-flux boundary condition was assigned to the upper boundary. The nodes representing the right and lower left (the boundary between the drywell and the bottom boundary) sides of the flow domain were set to no flux boundaries. The nodes at the bottom boundary ($z = -60$ m) were assigned a free drainage boundary condition (i.e., the water table was assumed to be far below this point). Note that the numerical experiments in this study do not account for the effect of the water table and future site-specific analysis and modeling studies are therefore warranted. Justification for the constant head condition is given in section 1 of the

SI. To represent a continuously full drywell, the total head ($H=h+z$) at the left boundary (at z = −8 to −38) was constant and equal to 0 m, i.e., the pressure head decreased linearly with depth from 38 m at the bottom boundary of the drywell to 8 at the top (Fig. 1). The initial condition (IC) in the flow domain was specified in terms of the soil water pressure head $h(x, z)$ and was set to a constant pressure head of −0.5 m (Fig. 1). This initial condition is justified because the bottom of the drywell at Fort Irwin is approximately 25 m from the water table. In addition, the water retention curve for the Fort Irwin soil (Fig. S4) shows that at −50 cm pressure head the corresponding water content (0.06) is close to the residual water content (0.043, Table 1) of the Fort Irwin soil. Therefore, we choose this relatively low ICs to make the change in storage smaller and to estimate recharge accurately within the simulation time.

3. NUMERICAL EXPERIMENTS

3.1 Homogeneous Domain

Numerical experiments (Experiment I, Table 2) were conducted to determine the values of I, R, and r_x under the Sand (S), Loamy Sand (LS), Sandy Loam (SL), Loam (L), and Silt (Si) soil materials for 365 days (1 year). A homogeneous flow domain was considered in these simulations and the hydraulic parameters for various soil textures were taken from the HYDRUS (2D/3D) Soil Catalog (Table 2). The value of I was collected over time during the simulation as the total volume of water infiltrated from the full drywell (i.e., the constant total head boundary). Similarly, the value of R was calculated as the volume of water drained through the bottom free drainage boundary. The radius of recharge was calculated from the saturated nodes and its corresponding distance in the x-direction at the bottom boundary of the flow domain. Note that all this information was available in output files of the HYDRUS (2D/3D) software.

3.2 Heterogeneous Domain

The previous experiment considered idealized homogeneous soil systems. However, most field-scale soil profiles are highly heterogeneous as shown in the Fort Irwin case study (section 1 in SI), and the hydraulic parameters may change over short distances. Natural geologic processes tend to produce layers and lenses in soil texture that form parallel to the soil surface (Phillips and Lorz, 2008). In addition, preferential water flow pathways can occur in the vertical direction as a result of: unstable flow behavior; dynamic capillary properties; macropores from decaying plant roots, burrowing earthworms, and animals; spatial variations in soil structure; and cracks in clayey soils; and fractured rocks (Flury et al., 1994; Hencher et al., 2011; Hendrickx and Flury, 2001; Phillips and Lorz, 2008; Sidle et al., 2000; Smith et al., 2008; Uchida et al., 2003; USDA, 2016). This study did not explicitly investigate the effect of preferential flow pathways and macropores, which has been extensively explored in previous research (Kung, 1990; Larsbo et al., 2005; Nativ et al., 1995; Šim nek and Bradford, 2008; Wood et al., 1997).

Several approaches such as univariate, multivariate, and multiple-point geostatistical techniques can be used to represent geometrical features and quantify soil variability (Elkateb et al., 2003; Jackson and Caldwell, 1993; Meerschman et al., 2013). In this study,

high permeable horizontal and vertical soil layers/lenses are represented using the Miller-Miller similitude geostatistical approach, which has been widely used in previous research (Feyen et al., 1998; Roth, 1995; Roth and Hammel, 1996; Sasidharan et al., 2019; Vereecken et al., 2007). The original Miller-Miller concept of scaling is based on using the scaling factor to adjust the degree of magnification or reduction of the K_s and h relative to a standard (reference) value (J. Šimůnek, 2012). The HYDRUS (2D/3D) computer software has an option to generate stochastic distributions of hydraulic conductivity (a_K) and pressure head (a_h) scaling factors using the Miller-Miller similitude approximation (Miller and Miller, 1956), which links these two scaling factors as follows: $a_K = a_h^{-2}$. In this study lognormal distribution for the scaling factors were employed (Šimůnek et al., 2007). Three input parameters: the standard deviation (σ) of $\log_{10}(a_K)$, and its correlation length in the lateral (the X-correlation length, X) and vertical (the Z-correlation length, Z) directions, were used to generate the stochastic field. The value of σ determines the extent of variations in the scaling factors, with higher values leading to higher variations in scaling factors. The correlation length is a measure of how similar the scaling factors are in a specific direction and to what distance. A high value of the X-correlation length means that the scaling factor maintains similar values for a greater horizontal distance. The same applies to the Z-correlation length in the vertical direction (Rassam et al., 2003). Procedures for generating autocorrelated or uncorrelated scaling factor fields and the original algorithm used in HYDRUS have been described in detail in the literature (El-Kadi, 1986; Freeze, 1975; Mejía and Rodríguez-Iturbe, 1974).

Soil hydraulic parameters (K_s, a, θ_r, θ_s, and n) for stochastic simulations were obtained from experiments conducted at the Fort Irwin site (Experiment II, Table 2). In particular, inverse optimization of falling head experimental data was used to obtain K_s and a (Sasidharan et al., 2018a), whereas other parameters (θ_r, θ_s, and n) were obtained from the measured particle size distribution (silt-clay-fraction) and the Rosetta software (Schaap et al., 2001; Segal et al., 2009).

Constant head drywell simulations in heterogeneous domains were used to determine I and R after 365 days. Multiple realizations of the stochastic parameters were employed to determine mean values of I (μI) and R (μR) and associated standard deviations. The computational time and cost to conduct these recharge simulations were large. To minimize these factors only ten realizations were considered for each stochastic heterogeneity parameter combination. The justification for using 10 realizations is given in our previous research (Sasidharan et al., 2019). In particular, these authors found that the mean and standard deviation of cumulative infiltration volume in heterogeneous soil profiles stabilized after around ten realizations for stochastic parameters considered in the present study. In this study, the following hypothetical combinations of the scaling factors with variable σ (σ=0.25, 0.5, 1: when X=l m and Z=0.1 m), X (X=0.1, 1, 10 m when σ=1 and Z=0.1 m), and Z (Z=0.1, 1,2 m when σ=1 and X=1) were used. Similar parameter ranges have been measured in the field (Freeze, 1975; Sudicky and MacQuarrie, 1989) and employed in previous modeling studies (Sasidharan et al., 2019). In addition, a simulation for a homogenous domain with the Fort Irwin soil hydraulic parameters was conducted to compare the μI and μR between homogeneous and heterogeneous domains.

The times when the first (i.e., early arrival time, EA_T) and last (i.e., late arrival time, LA_T) bottom boundary nodes got saturated for the first and last times were extracted from the output data file with nodal water contents from each HYDRUS (2D/3D) simulation. Similarly, the first (i.e., the early arrival point, EA_P) and last (i.e., the late arrival point, LA_P) bottom boundary nodes that were saturated were also calculated. A mean radius of recharge (r_x) was calculated as the distance in the x-direction between the first and last nodes at the bottom boundary that were fully saturated at the end of the 365 days simulation. Mean parameter values and 95%-Confidence Intervals (CI) were calculated for all parameters from ten simulations.

4.   RESULT AND DISCUSSIONS

4.1.   Homogeneous Soil Profiles

Numerical experiments were conducted to better understand the transient relationship between the cumulative infiltration and recharge volumes in homogeneous soil domains. Simulations considered higher permeability soils (e.g., S, LS, SL, L, and Si) that are generally used for vadose zone infiltration devices. Figs. 2A and 2B show simulated water content (θ) profiles in various soils (e.g., S, LS, SL, L, and Si) after 0.73 and 365 days, respectively. Fig. 3 presents corresponding information about the infiltration and recharge behavior in these same simulations. The width and depth of the cone of infiltration after 0.73 days (Fig. 2A) decreases with a decrease in the soil K_s in the order S, LS, SL, L, and Si (Table 1). Similarly, the value of I as a function of time increases with the soil K_s (Fig. 3A).

The recharge at a specific time depends on changes in the soil hydraulic properties with θ (van Genuchten et al., 1991) and the radius of the cone of infiltration at the bottom boundary (r_x). Yeh et al. (1985a) and Yeh et al. (1985b) demonstrated that the variability of capillary pressure or moisture content increases when the mean capillary pressure increases, and the anisotropy ratio (vertical/horizontal) of the effective unsaturated K_s increases when the mean capillary pressure increases or mean moisture content decreases. Coarser soils (e.g., sand) with larger pore sizes have lower θ and $K(\theta)$ (hydraulic conductivity at varying water saturation) values before the wetting front arrives (Fig. S5A). Consequently, the background θ (Fig. 2) and the initial recharge rate (Fig. 3B) is lower in coarser than finer textured soils. However, coarser soils also have higher values of $K(\theta)$ when θ approaches saturated conditions (Fig. S5B). The wetting front, therefore, arrives at the bottom boundary faster in coarser than finer textured soils (in 0.8 days for sand compared to 16.7 days for silt) and this is associated with a dramatic increase in R (Fig. 3B) and r_x (Fig. 3C). At the end of the simulation (365 days), the cones of infiltration (Fig. 2B) are similar and r_x=21.5 m (Fig. 3C) for various soil types and the final value of R increases with the soil K_s (Fig. 3B).

Fig.3D shows plots of I versus R at 365 day for the simulations in various soils. Note that a large volume of water needs to infiltrate into the soil before recharge from the drywell rapidly increases. Furthermore, this delay in recharge increases for coarser textured soils that have lower background values of θ. For example, recharge rapidly increased when I=9526 m^3 for sand compared to I=1896 m^3 for silt. This occurs because infiltrating water needs to fill more of the pore space in coarser (lower initial θ) than in finer textured soils before the cone of infiltration can reach the bottom boundary. These simulation results will be sensitive

to the model's initial conditions. In this work, we have assumed an initial head of −0.5 m throughout the domain. Note that the simulated I=1896-9526 m^3 can have a resemblance to an actual arid- or semi-arid site like Fort Irwin, which received 515 m^3 input water from irrigation runoff during 200 days monitoring period (summer).

4.2. Heterogeneous Soil Profiles

4.2.1. Cumulative Infiltration and Recharge—The above simulations were highly idealized because they considered homogeneous soil profiles. In contrast, natural subsurface is inherently heterogeneous. However, previous studies (Hencher et al., 2011; Phillips and Lorz, 2008; Sasidharan et al., 2019; Sidle et al., 2000; Smith et al., 2008; Uchida et al., 2003; USDA, 2016) and the case study presented in the SI demonstrates that layered soil structures are very common. Illustrative simulations were therefore conducted to better understand the effects of stochastic heterogeneity parameters (X, Z, and σ) for K_s on the cumulative infiltration and recharge volumes from a drywell. Figs. 4 and 5 show representative h and θ distributions, respectively, after 365 days constant head simulation in homogeneous (Figs. 2A and 3A) and stochastic (Figs. 2B–2H and 3B–3H) domains. The Fort Irwin soil hydraulic parameters (Experiment II, Table 1) were employed in these simulations, and stochastic parameters equaled X=10 m, Z=0.1 m, and σ=1 in Fig. 4B and 5B; X=1 m, Z=0.1 m, and σ=1 in Fig. 4C and 5C; X=0.1 m, Z=0.1 m, and σ=1 in Fig. 4D and 5D; X=1 m, Z=1 m, and σ=1 in Fig. 4E and 5E; X=1 m, Z=2 m, and σ=1 in Fig. 4F and 5F; X=1 m, Z=0.1 m, and σ=0.5 in Fig. 4G and 5G; and X=1 m, Z=0.1 m, and σ=0.25 in Fig. 4H and 5H. Heterogeneous domains display wider distributions (in the lateral direction) of the saturated area and the presence of unsaturated pockets within the cone of infiltration compared to a homogeneous domain (Figs. 4A and 5A).

Fig. 6 shows values of μI and μR, and their 95%-CI after 365 days as a function of σ (Fig. 6A), X (Fig. 6B), and Z (Fig. 6C). Specific stochastic parameters that were employed in these simulations included: σ=0.25, 0.5, and 1 when X=1 m and Z=0.1 m in Fig. 6A; X=0.1, 1, 10 m when Z=0.1 m and σ=1 in Fig. 6B; and Z=0.1, 1,2 m when X=1 m and σ=1 in Fig. 6C. Fig. 6 also includes values of I and R after 365 days for the corresponding homogeneous domain. A comparison of results for homogeneous and heterogeneous simulations reveals that both infiltration and recharge were higher for heterogeneous domains. Consequently, simulations that employ a homogenous domain will always underestimate the actual infiltration and recharge efficiency of a drywell. The heterogeneous simulations indicate that the value of μR will always be smaller than μI during the short-term experiment. This revealed that over the 365 days simulation period, not all infiltrated water will recharge groundwater because some of the water will be trapped in isolated pockets or high permeable regions surrounded by low permeable layers (Figs. 4 and 5).

The distribution and volume of trapped water in the flow domain will be highly dependent on the subsurface heterogeneity. Fig. 6 shows that μI and μR tended to increase with σ (Fig. 6A) and X (Fig. 6B) but decreased with Z (Fig. 6C) due to differences in the water distribution (Figs. 4 and 5). Fig. 7 shows a similar dependence of the mean value of r_X at the bottom boundary on σ (Fig. 7A), X (Fig. 7B), and Z (Fig. 7C). An increase in σ leads to the formation of more permeable regions, which enhance infiltration (Fig 6A), recharge (Fig.

6A), and spreading (Fig. 7A). Similarly, an increase in X produces larger lateral lenses with high permeability that enhance the rapid movement of the wetting front in the horizontal direction (Figs. 5D, 5C, and 5B) and facilitate the infiltration and recharge of water over a larger area (Fig. 6B and 7B). Conversely, an increase in Z creates larger vertical lenses with high permeability, which facilitates the rapid vertical movement of water over a relatively small area (Figs. 5E, 5F, 6C, and 7C). The 95% CIs for μI and μR were sometimes very large in Fig. 6, especially for the highest values of X and Z in Figs. 6B and 6C, respectively. This uncertainty reflects differences in the continuity of the high permeability regions and the area of recharge (Fig. 7). Several other studies have reported extensive lateral (horizontal) moisture movement but a limited vertical movement in different systems (Mantoglou and Gelhar, 1987; Routson et al., 1979; Sinai et al., 1974; Yeh et al., 1985a; Yeh et al., 1985b). However, these general findings only give information regarding the long-term trend of infiltration and recharge, and do not consider the presence of high permeable horizontally and vertically correlated soil layers. Therefore, it is important to understand the infiltration and recharge behavior, the arrival time and arrival location during short-term drywell operation to establish a site-specific monitoring system.

4.2.2 Time and Location of Recharge—The drywell regulatory guidelines require a mandatory separation distance of only 1.5-13 m between the drywell and the local groundwater table to provide a contaminant treatment zone (City of Portland, 2008; City of Portland, 2015; EPA, 1999; Washington State Department of Ecology, 2006). However, soils with highly permeable vertical lenses or fractures could minimize the contaminant treatment time and can produce an early arrival of contaminants such as pathogenic microbes to groundwater (Bradford et al., 2017; Mohanty et al., 2016; Wang et al., 2014a; Wang et al., 2014b). Figs. 4–7 examined infiltration and recharge from a drywell in heterogeneous and homogeneous soils after 365 days under constant head conditions. Values of the mean final recharge rate (μr) and mean r_x in Fig. 7 can be used to estimate the average yearly recharge flux to groundwater from a drywell (i.e., μr divided by πr_x^2) for a constant head condition (Fig. S6). This information is vital for determining the average yearly Darcy velocity during recharge for conservatively transported contaminants during recharge. However, it does not address variability in the recharge behavior with time or the location on the bottom boundary. Simulation results were therefore further evaluated to address these issues. This information has important implications for properly determining times and locations for assessing the potential migration of contaminants through the vadose zone to the groundwater table.

Fig. 8 provides summary information about recharge with time and location for stochastic simulations when X=1 m, Z=0.1 m, and σ=0.25, 0.5, and 1. The early (EA_T) and late (LA_T) mean arrival times decreased with σ in Figs. 8A and 8B, respectively. However, the mean location for early (EA_P) and late (LA_P) arrival point increased with σ (Figs. 8C and 8D). Observed differences in the early and late arrival times and points can be explained by analyzing the μR data with time (Figs. 8E and 8F). There was a significant delay in recharge when σ=0.25 (compared to higher as) (Fig. 8E) and the value of μR was very close to that for the homogeneous soil at 365 days (Fig. 8). A small value of σ leads to a more uniform and lower permeability, and a cone of infiltration that takes longer to fill before the wetting

front arrives at the bottom boundary. An increase in σ creates more high permeability zones that decrease the early and late arrival times. It also increases the spreading of water (Fig. 4H, 4G, 4D, and 7A) and thereby increases the distance to the early and late arrival points. Interestingly, all 4 parameters (EA_T, LA_T, EA_P, LA_P) showed a large 95%-CIs due to differences in the predicted water distributions.

Fig. 9 provides summary information about recharge with time and location for stochastic simulations when Z=0.1 m, σ=1, and X=0.1, 1, 10 m. Figs. 9A, 9B, 9C, and 9D show values of EA_T, LA_T, EA_P, and LA_P, respectively, and their corresponding 95%-CIs that increase with the X-correlation length. These trends reflect increasing water spreading with X due to larger lenses in the lateral direction with high permeability. Figs. 9E and 9F show values of μR as a function of time during early (i.e., <75 days) and late (i.e., <365 days) stages, respectively. Early stages of recharge show a decrease in μR with an increase in X because recharge is delayed by increasing lateral spreading. This trend is consistent with the results displayed in Figs. 9A–9D. Conversely, μR was greatest when X=10 m at later stages of recharge (Fig. 9F). This suggests that vertical migration and recharge was enhanced once larger horizontal lenses with higher permeability were filled. In this case, higher values of θ and $K(\theta)$ were achieved in high permeability lenses that enhanced recharge.

Previous researchers have similarly reported that the vertical effective K_s is small and the lateral effective K_s is large in the wetting front of stratified soil (Mantoglou and Gelhar, 1987), which increased the lateral movement of contaminants in the unsaturated zone below various waste disposal facilities (Crosby III et al., 1968; Crosby III et al., 1971; Palmquist and Johnson, 1962; Price et al., 1979; Prill, 1977). Enhanced lateral movement can be attributed to the fact that at high tension the hydraulic conductivity of fine-textured materials is relatively high, and water may prefer to spread laterally in a fine bed than to move vertically through coarser ones (Routson et al., 1979). In natural environments, layered soil profiles with high permeable sand layers followed by low permeable clay lenses with extensions and thicknesses of several tens to hundreds of meters can be present (Phillips and Lorz, 2008). Trauntwein et al. (1983) investigated wastewater movement from an evaporation pond in the stratified unsaturated zone and observed that the contamination pool extended laterally to a distance of 2000 m due to the formation of a saturated perched water zone above the water table. The presence of such geological formations (e.g., clay layer at Fort Irwin, SI) could delay groundwater recharge from a drywell from 1 to 100+ years. Therefore, the presence of a high permeable soil around the drywell infiltration area may not contribute to groundwater recharge for many years.

Fig. 10 provides summary information about recharge with time and location for stochastic simulations when X=1 m, σ=1, and Z=0.1, 1, and 2 m. Figs. 10A and 10B show that the values of EA_T and LA_T, respectively, decreased with Z. Conversely, values of EA_P and LA_P increased (Fig. 10C) and decreased (Fig. 10D) with Z. Fig. 10E shows that values of μR during the early stage (<75 days) increased with Z. Among all stochastic parameter combinations, the X=1, Z=2, σ=1 simulation had the earliest arrival time (34±12 days). The presence of highly permeable vertical lenses facilitates the faster downward movement of water and thus an early arrival time (Fig. 10A). However, the value of μR during the late stage (<365 days) was greatest when Z=0.1 m and lowest when Z=2 m (Fig. 10F). In this

case, the presence of a thick vertical lens (Fig. 10F) when $Z=2$ m reduced the overall width of the cone of infiltration (Figs. 4 and 5) and the recharge area (Fig. 7), and this decreased the long-term value of μR. All 4 parameters showed a large 95%-CIs for simulations shown in Fig. 10 and this reflects the variability in water distributions and flow rates.

Groundwater monitoring wells are commonly installed a few meters away from a drywell (Hamad et al., 2016; Izuka, 2011). Previous stochastic theory studies (Mantoglou and Gelhar, 1987; Yeh et al., 1985a; Yeh et al., 1985b) predicts that a contamination plume tends to spread laterally in dry vadose zone soils, while vertical movement is slow. Contaminants may, therefore, arrive at the water table much later than is predicted by many classic one-dimensional models. However, this study demonstrated that the arrival time could range from 33-317 days and the arrival location could be 0.1-44 m away from the bottom releasing point of a drywell depending on the heterogeneity. If the location of a monitoring well and the sampling timing are not properly selected, then the recharge water quality can lead to a misinterpretation of the anticipated transport and risks from contaminants. Consequently, the use of model projections for estimating the magnitude of groundwater recharge and transport of contaminants from drywells in heterogeneous subsurface conditions will likely have a high degree of uncertainty. One should, therefore, be cautious when determining the risks from drywells during the short-term operation at a site that is not thoroughly characterized.

Based on the modeling realizations, the value of μR was always smaller for a homogeneous than a heterogeneous domain (Figs. 8F, 9F, and 10F). Previously, Sasidharan et al. (2018a) found that an equivalent homogeneous soil domain could be used to accurately predict μI for a heterogeneous soil domain. The sensitivity of a modeled recharge volume to various physical configurations and connectivity of soil hydraulic properties implies that measurement of the soil heterogeneity below the drywell is an important consideration when evaluating the potential for groundwater recharge. As shown in Fig. S7, the correlation between drywell infiltration and the recharge volume can be highly non-linear for heterogeneous soil domains. Thus, model estimates of short- or long-term recharge efficiencies may not be reliable when constrained solely by the inferred volume of infiltration based on empirical measurements within a drywell system.

5. CONCLUSIONS AND FUTURE IMPLICATIONS

Drywells are widely used to capture stormwater and convey it to the vadose zone for subsequent groundwater recharge. However, assessing the performance of a drywell and its recharge efficiency over the short- or long-term is very tedious, time-consuming, expensive, and complex. To successfully install a drywell, conduct groundwater monitoring, and collect accurate groundwater quality information requires a careful design of field experiments and a knowledge of the subsurface heterogeneity in soil hydraulic properties.

Numerical experiments were conducted to understand the relationship between the cumulative infiltration and recharge volumes in the homogeneous (S, LS, SL, L, and Si) soil domains. The cumulative infiltration and recharge volumes increased with K_s. During the initial stages of infiltration, the coarser textured sandy soil had a lower background θ and, therefore, a large volume of water had to infiltrate before the recharge rate from the drywell

rapidly increased. The wetting front arrived at the bottom boundary faster in coarser than finer-textured soils. However, all soil types had a similar value of the recharge area radius at the end of the simulation. Note that this may not occur when the model is run with a more representative transient loading condition. Groundwater monitoring well installations placed at the outer radius of the recharge area may therefore not be the best choice.

Homogeneous soil profiles are highly idealized conditions compared to natural subsurface soils that are highly heterogeneous. Therefore, additional numerical experiments were conducted to better understand the influence of stochastic heterogeneity in soil hydraulic properties on drywell infiltration and recharge behavior. The cumulative infiltration and recharge volume after a 365 days constant head simulation were higher for heterogeneous domains than for the homogeneous domain. However, the cumulative recharge volume was smaller than the cumulative infiltration volume, and their correlations were highly non-linear. This result indicates that a fraction of infiltrated water can be trapped in isolated pockets or highly permeable regions in the vadose zone and the knowledge of the infiltration volume under varying stormwater flow events may not be a reliable predictor of potential short-term recharge. Both cumulative infiltration and recharge increased with increasing σ and the lateral correlation length but decreased with an increasing vertical correlation length. The radius of recharge at the bottom boundary showed a similar dependency on stochastic parameters.

The mean early and late arrival times decreased with σ, whereas the mean early and late arrival points increased with σ. An increase in σ creates more high permeability and connectivity zones and increases the spreading of water. The values of both early and late arrival times and locations increased with the X-correlation length. The presence of larger, highly permeable lateral lenses increases the spreading of water. At the same time, values of early and late arrival times decreased with the Z-correlation length. In contrast, early and late arrival locations increased and decreased with Z, respectively. The presence of highly permeable vertical lenses facilitates the faster downward moment of water but reduces the overall width of the cone of filtration and the recharge area.

This research points out that the assumption of a highly permeable homogenous soil around the drywell may result in unrealistic model estimates of recharge to groundwater. Some understanding of the hydraulic properties, subsurface heterogeneity, and its continuity between the drywell and the groundwater table is essential for making an informed decision on recharge and contaminant transport. The current drywell infiltration tests performed by contractors are very simple and fail to capture accurately the hydraulic behavior of a site. Therefore, carefully planned falling head and constant head (multiple cycles) experiment should be conducted in a newly installed drywell and effective hydraulic properties can be obtained by the inverse optimization of the observed data (Sasidharan et al., 2018a; Sasidharan et al., 2019). In the absence of extensive knowledge about the subsurface heterogeneity, an equivalent homogeneous domain with inversely optimized stochastic parameters can be used to estimate the cumulative infiltration (Sasidharan et al., 2019), even if such an analysis may not provide an accurate estimation of recharge under transient conditions.

This research demonstrated the importance of subsurface heterogeneity on recharge from drywells. However, it is important to recognize the limitations and assumptions employed in this study. The consideration of heterogeneous subsurface and subsequent data analysis can be time-consuming and adds a lot more complexity. For example, a maximum X-correlation length of 10 m was considered in this study due to the limitation in the size of the model simulation domain size and the associated simulation time and cost. The stochastic input parameters used in the numerical experiments were hypothetical (since site-specific data is not available) and initial and boundary conditions were chosen based on the limited knowledge available from Fort Irwin's study site.

It is recommended that hydrogeologists, drywell practitioners, and regulators implement new strategies during drywell installation to collect detailed site-specific subsurface heterogeneity data for future validation studies. For example, drywell performance could be assessed using single or multiple slanted boreholes that are instrumented with water content probes and solution sampling ports at several depths to track water content profiles and contaminant migration, respectively (Dahan et al., 2009). Such information can help to quantify the influence of subsurface heterogeneity on recharge and serve as an early warning system of contaminant migration in the vadose zone (Dahan et al., 2009). In addition, a variety of near-surface geophysical techniques can provide valuable information on site structure, hydrology and hydrogeology, and contamination plume information (Annan, 2005; Binley and Kemna, 2005; Cassiani et al., 2014; Everett and Meju, 2005; Revil et al., 2006). However, these sophisticated academic methods and techniques are often not feasible given real-world limits on time, cost, and data availability, especially for risk and uncertainty analyses. Therefore, academics and practitioners should collaborate to develop qualitative methods for drywell optimization and risk assessment (Bode et al., 2018). If site-specific data are not available for a given subsurface, literature values of similar systems can in principle be used for an initial assessment (Schilling et al., 2017).

The Fort Irwin drywell case study demonstrated that urban and rural areas in the arid or semi-arid environment may still receive regular input of water from urban runoff and can be used as an alternative source of infiltration water. Such a scenario will lead to a constant head boundary condition within the drywell and will act as an upper bound for groundwater recharge and as a worst-case scenario for the contaminant transport. Therefore, this study only considered constant head boundary conditions to understand the effect of stochastic parameters on cumulative infiltration and recharge volumes, the area of recharge, arrival time, and arrival location of infiltrated water from a drywell. Additional research is needed to study the influence of natural weather conditions such as rain frequency and intensity at a drywell site. Episodic rainfall events create transient boundary conditions in the drywell that will add more complexity to recharge estimates and risk assessment. This topic will be addressed in a future paper.

Supplementary Material

Refer to Web version on PubMed Central for supplementary material.

ACKNOWLEDGMENT

9. REFERENCE

Allison G, Gee G, Tyler S, 1994 Vadose-Zone Techniques for Estimating Groundwater Recharge in Arid and Semiarid Regions. Soil Science Society of America Journal, 58(1): 6–14.

Annan AP, 2005 GPR Methods for Hydrogeological Studies, Hydrogeophysics. Springer, pp. 185–213.

Arnaud E, Best A, Parker BL, Aravena R, Dunfield K, 2015 Transport of through a Thick Vadose Zone. Journal of Environmental Quality, 44(5): 1424–34. DOI:10.2134/jeq2015.02.0067 [PubMed: 26436260]

Binley A, Kemna A, 2005 Dc Resistivity and Induced Polarization Methods, Hydrogeophysics. Springer, pp. 129–156.

Bode F, Ferré T, Zigelli N, Emmert M, Nowak W, 2018 Reconnecting Stochastic Methods with Hydrogeological Applications: A Utilitarian Uncertainty Analysis and Risk Assessment Approach for the Design of Optimal Monitoring Networks. Water Resources Research, 54(3): 2270–2287. DOI:10.1002/2017wr020919

Bradford SA, Leij FJ, Schijven J, Torkzaban S, 2017 Critical Role of Preferential Flow in Field-Scale Pathogen Transport and Retention. Vadose Zone Journal, 16(4). DOI:10.2136/vzj2016.12.0127

Brunetti G, Šimůnek J, Turco M, Piro P, 2017 On the Use of Surrogate-Based Modeling for the Numerical Analysis of Low Impact Development Techniques. Journal of Hydrology, 548: 263–277. DOI:10.1016/j.jhydrol.2017.03.013

Cadmus, 1991 Storm Water Drainage Wells (5d2), Waltham, MA.

Cadmus, 1996 Storm Water Drainage Well Guidance - Draft, Waltham, MA.

Cadmus, 1999 State-by-State Notebooks Compiling Results from the Class V Underground Injection Control Study, United States Environmental Protection Agency.

Camesano TA, Logan BE, 1998 Influence of Fluid Velocity and Cell Concentration on the Transport of Motile and Nonmotile Bacteria in Porous Media. Environmental Science and Technology, 32(11): 1699–1708.

Carsel RF, Parrish RS, 1988 Developing Joint Probability Distributions of Soil Water Retention Characteristics. Water Resources Research, 24(5): 755–769.

Cassiani G, Binley A, Kemna A, Wehrer M, Orozco AF, Deiana R, Boaga J, Rossi M, Dietrich P, Werban U, Zschomack L, Godio A, JafarGandomi A, Deidda GP, 2014 Noninvasive Characterization of the Trecate (Italy) Crude-Oil Contaminated Site: Links between Contamination and Geophysical Signals. Environmental Science and Pollution Research, 21(15): 8914–31. DOI: 10.1007/s11356-014-2494-7 [PubMed: 24619658]

City of Portland., 2008 Decision Making Framework for Groundwater Protectiveness Demonstrations, City of Portland, Bureau of Environmental Services.

City of Portland., 2015 Underground Injection Control Management Plan, City of Portland, Bureau of Environmental Services.

Crosby JW III, Johnstone DL, Drake CH, Fenton RL, 1968 Migration of Pollutants in a Glacial Outwash Environment. Water Resources Research, 4(5): 1095–1114.

Crosby JW III, Johnstone DL, Fenton RL, 1971 Migration of Pollutants in a Glacial Outwash Environment, 3. Water Resources Research, 7(3): 713–720.

Dahan O, Talby R, Yechieli Y, Adar E, Lazarovitch N, Enzel Y, 2009 In Situ Monitoring of Water Percolation and Solute Transport Using a Vadose Zone Monitoring System. Vadose Zone Journal, 8(4): 916–925. DOI: 10.2136/vzj2008.0134

Dillon P, 2005 Future Management of Aquifer Recharge. Hydrogeology Journal, 13(1): 313–316. DOI: 10.1007/s10040-004-0413-6

Dillon P, Stuyfzand P, Grischek T, Lluria M, Pyne R, Jain R, Bear J, Schwarz J, Wang W, Fernandez E, 2019 Sixty Years of Global Progress in Managed Aquifer Recharge. Hydrogeology Journal, 27(1): 1–30.

Edwards EC, Harter T, Fogg GE, Washburn B, Hamad H, 2016 Assessing the Effectiveness of Drywells as Tools for Stormwater Management and Aquifer Recharge and Their Groundwater Contamination Potential. Journal of Hydrology, 539: 539–553. DOI:10.1016/j.jhydrol.2016.05.059

El-Kadi AI, 1986 A Computer Program for Generating Two-Dimensional Fields of Autocorrelated Parameters. Groundwater, 24(5): 663–667.

Elkateb T, Chalaturnyk R, Robertson PK, 2003 An Overview of Soil Heterogeneity: Quantification and Implications on Geotechnical Field Problems. Canadian Geotechnical Journal, 40(1): 1–15.

EPA, 1999 The Class V Underground Injection Control Study, United States Environmental Protection Agency, Office of Ground Water Drinking Water.

Ercin AE, Hoekstra AY, 2014 Water Footprint Scenarios for 2050: A Global Analysis. Environ Int, 64: 71–82. DOI:10.1016/j.envint.2013.11.019 [PubMed: 24374780]

Everett ME, Meju MA, 2005 Near-Surface Controlled-Source Electromagnetic Induction, Hydrogeophysics. Springer, pp. 157–183.

Feng W, Zhong M, Lemoine JM, Biancale R, Hsu HT, Xia J, 2013 Evaluation of Groundwater Depletion in North China Using the Gravity Recovery and Climate Experiment (Grace) Data and Ground-Based Measurements. Water Resources Research, 49(4): 2110–2118.

Feyen J, Jacques D, Timmerman A, Vanderborght J, 1998 Modeling Water Flow and Solute Transport in Heterogeneous Soils: A Review of Recent Approaches. Journal of Agricultural Engineering Research, 70(3): 231–256. DOI:10.1006/jaer.1998.0272

Flury M, Flühler H, Jury WA, Leuenberger J, 1994 Susceptibility of Soils to Preferential Flow of Water: A Field Study. Water Resources Research, 30(7): 1945–1954.

Freeze RA, 1975 A Stochastic-Conceptual Analysis of One-Dimensional Groundwater Flow in Nonuniform Homogeneous Media. Water Resources Research, 11(5): 725–741.

Gale I, 2005 Strategies for Managed Aquifer Recharge (Mar) in Semi-Arid Areas. UNESCO.

Gray DM, Norum D, 1967 The Effect of Soil Moisture on Infiltration as Related to Runoff and Recharge, Proceedings of Hydrology Symposium. Citeseer.

Hamad HLHBAAP, Nelso N; Green Rebecca.; Edwards Emily.; Washburn Barbara., 2016 Dry Wells and the Risk of Contamination: An Annotated Bibliography, Environmental Protection Agency, Pesticide & Environmental Toxicology Branch Office of Environmental Health Hazard Assessment California.

Hammel K, Roth K, 1998 Approximation of Asymptotic Dispersivity of Conservative Solute in Unsaturated Heterogeneous Media with Steady State Flow. Water Resources Research, 34(4): 709–715.

Haney J, Leach M, Sobchak L, 1989 Dry Wells – Solution or Pollution?, Arizona Department of Environmental Quality, Phoenix, Arizona.

Hencher SR, Lee SG, Carter TG, Richards LR, 2011 Sheeting Joints: Characterisation, Shear Strength and Engineering. Rock Mechanics and Rock Engineering, 44(1): 1–22. DOI: 10.1007/ s00603-010-0100-y

Hendrickx JM, Flury M, 2001 Uniform and Preferential Flow Mechanisms in the Vadose Zone. Conceptual Models Of Flow And Transport In The Fractured Vadose Zone: 149–187.

Hendrickx JM, Walker GR, 2017 Recharge from Precipitation, Recharge of Phreatic Aquifers in (Semi-) Arid Areas. Routledge, pp. 19–111.

Huang T, Pang Z, Liu J, Yin L, Edmunds WM, 2017 Groundwater Recharge in an Arid Grassland as Indicated by Soil Chloride Profile and Multiple Tracers. Hydrological Processes, 31(5): 1047–1057.

Izuka SK, 2011 Potential Effects of Roadside Dry Wells on Groundwater Quality on the Island of Hawai'i—Assessment Using Numerical Groundwater Models, U.S. Geological Survey.

Šim nek J, M.T.v.G.a.M.Š., 2012 The Hydrus Software Package for Simulating the Two- and Three-Dimensional Movement of Water, Heat, and Multiple Solutes in Variably-Saturated Porous Media, Technical Manual, Version 2.0.

Jackson R, Caldwell M, 1993 Geostatistical Patterns of Soil Heterogeneity around Individual Perennial Plants. Journal of Ecology: 683–692.

Johnson WP, Blue KA, Logan BE, Arnold RG, 1995 Modeling Bacterial Detachment During Transport through Porous Media as a Residence-Time-Dependent Process. Water Resources Research, 31(11): 2649–2658.

Kung KJS, 1990 Preferential Flow in a Sandy Vadose Zone: 2. Mechanism and Implications. Geoderma, 46(1–3): 59–71. DOI:10.1016/0016-7061(90)90007-v

Larsbo M, Roulier S, Stenemo F, Kasteel R, Jarvis N, 2005 An Improved Dual-Permeability Model of Water Flow and Solute Transport in the Vadose Zone. Vadose Zone Journal, 4(2): 398–406. DOI:10.2136/vzj2004.0137

Mancosu N, Snyder R, Kyriakakis G, Spano D, 2015 Water Scarcity and Future Challenges for Food Production. Water, 7(3): 975–992.

Mantoglou A, Gelhar LW, 1987 Effective Hydraulic Conductivities of Transient Linsaturated Flow in Stratified Soils. Water Resources Research, 23(1): 57–67.

Meerschman E, Van Meirvenne M, Van De Vijver E, De Smedt P, Islam MM, Saey T, 2013 Mapping Complex Soil Patterns with Multiple-Point Geostatistics. European Journal of Soil Science, 64(2): 183–191. DOI:10.1111/ejss.12033

Mejía JM, Rodríguez-Iturbe I, 1974 On the Synthesis of Random Field Sampling from the Spectrum: An Application to the Generation of Hydrologic Spatial Processes. Water Resources Research, 10(4): 705–711.

Mekonnen MM, Hoekstra AY, 2016 Four Billion People Facing Severe Water Scarcity. Sci Adv, 2(2): el500323 DOI:10.1126/sciadv.1500323

Michael E, 1997 St. Joseph County Health Dept. Letter to Alan Melcer, US Environmental Protection Agency, Underground Control Branch, Chicago, IL, Mishawaka, IN.

Miller E, Miller R, 1956 Physical Theory for Capillary Flow Phenomena. Journal of Applied Physics, 27(4): 324–332.

Min L, Shen Y, Pei H, 2015 Estimating Groundwater Recharge Using Deep Vadose Zone Data under Typical Irrigated Cropland in the Piedmont Region of the North China Plain. Journal of Hydrology, 527: 305–315. DOI:10.1016/j.jhydrol.2015.04.064

Mohanty SK, Saiers JE, Ryan JN, 2016 Colloid Mobilization in a Fractured Soil: Effect of Pore-Water Exchange between Preferential Flow Paths and Soil Matrix. Environmental Science & Technology, 50(5): 2310–7. DOI:10.1021/acs.est.5b04767 [PubMed: 26829659]

Nativ R, Adar E, Dahan O, Geyh M, 1995 Water Recharge and Solute Transport through the Vadose Zone of Fractured Chalk under Desert Conditions. Water Resources Research, 31(2): 253–261. DOI:Doi 10.1029/94wr02536

Orr VJ, 1993 Wellhead Protection - Lessons Learned. Journal of Applied Ground Water Protection, Volume 1, Number 1.

Palmquist W, Johnson A, 1962 Vadose Flow in Layered and Nonlayered Materials. US Geological Survey Professional Paper, 450: 142–1L.

Phillips JD, Lorz C, 2008 Origins and Implications of Soil Layering. Earth-Science Reviews, 89(3–4): 144–155. DOI:10.1016/j.earscirev.2008.04.003

Postel SL, Daily GC, Ehrlich PR, 1996 Human Appropriation of Renewable Fresh Water. Science, 271(5250): 785–788.

Price S, Kasper R, Additon M, Smith R, 1979 Distribution of Plutonium and Americium beneath the 216-Z-1a Crib: A Status Report, Atomics International Div.

Prill RC, 1977 Movement of Moisture in the Unsaturated Zone in a Loess-Mantled Area, Southwestern Kansas, 1021 US Government Printing Office.

Rassam D, Šimůnek J, van Genuchten MT, 2003 Modelling Variably Saturated Flow with Hydrus-2d. ND Consult.

Revil A, Titov K, Doussan C, Lapenna V, 2006 Applications of the Self-Potential Method to Hydrological Problems, Applied Hydrogeophysics. Springer, pp. 255–292.

Richard SE, Peter D, 2017 Linking Groundwater and Surface Water: Conjunctive Water Management, Advances in Groundwater Governance. CRC Press, pp. 329–351.

Ries F, Lange J, Schmidt S, Puhlmann H, Sauter M, 2015 Recharge Estimation and Soil Moisture Dynamics in a Mediterranean, Semi-Arid Karst Region. Hydrology and Earth System Sciences, 19(3): 1439–1456.

Roth K, 1995 Steady State Flow in an Unsaturated, Two-Dimensional, Macroscopically Homogeneous, Miller-Similar Medium. Water Resources Research, 31(9): 2127–2140.

Roth K, Hammel K, 1996 Transport of Conservative Chemical through an Un saturated Two-Dimensional Miller-Similar Medium with Steady State Flow. Water Resources Research, 32(6): 1653–1663.

Routson R, Price W, Brown D, Fecht K, 1979 High-Level Waste Leakage from the 241-T-106 Tank at Hanford, Rockwell International Corp.

Sasidharan S, Bradford SA, Šimůnek J, De Jong B, S RK, 2018a Evaluating Drywells for Stormwater Management and Enhanced Aquifer Recharge. Advances in Water Resources, 116: 167–177. DOI:10.1016/j.advwatres.2018.04.003 [PubMed: 30245542]

Sasidharan S, Bradford SA, Šimůnek J, Kraemer SR, 2019 Drywell Infiltration and Hydraulic Properties in Heterogeneous Soil Profiles. Journal of Hydrology (Amst), 570: 598–611. DOI:10.1016/j.jhydrol.2018.12.073

Sasidharan S, Bradford SA, Šimůnek J, Torkzaban S, 2018b Minimizing Virus Transport in Porous Media by Optimizing Solid Phase Inactivation. Journal Of Environmental Quality, 47(5): 1058–1067. DOI:10.2134/jeq2018.01.0027 [PubMed: 30272798]

Sasidharan S, Bradford SA, Šimůnek J, Torkzaban S, Vanderzalm J, 2017a Transport and Fate of Viruses in Sediment and Stormwater from a Managed Aquifer Recharge Site. Journal of Hydrology, 555(Supplement C): 724–735. DOI: 10.1016/j.jhydrol.2017.10.062

Sasidharan S, Bradford SA, Torkzaban S, Ye X, Vanderzalm J, Du X, Page D, 2017b Unraveling the Complexities of the Velocity Dependency of E. Coli Retention and Release Parameters in Saturated Porous Media. The Science Of The Total Environment, 603-604: 406–415. DOI:10.1016/j.scitotenv.2017.06.091 [PubMed: 28641182]

Savenije HHG, 2000 Water Scarcity Indicators; the Deception of the Numbers. Phys Chem Earth PtB, 25(3): 199–204. DOI:Doi 10.1016/S1464-1909(00)00004-6

Scanlon BR, Reedy RC, Faunt CC, Pool D, Uhlman K, 2016 Enhancing Drought Resilience with Conjunctive Use and Managed Aquifer Recharge in California and Arizona. Environmental Research Letters, 11(3): 035013.

Schaap MG, Leij FJ, van Genuchten MT, 2001 Rosetta : A Computer Program for Estimating Soil Hydraulic Parameters with Hierarchical Pedotransfer Functions. Journal of Hydrology, 251(3–4): 163–176. DOI:10.1016/s0022-1694(01)00466-8

Schijven JF, Hassanizadeh SM, 2000 Removal of Viruses by Soil Passage: Overview of Modeling, Processes, and Parameters. Critical Reviews in Environmental Science and Technology, 30(1): 49–127.

Schilling OS, Irvine DJ, Hendricks Franssen HJ, Brunner P, 2017 Estimating the Spatial Extent of Unsaturated Zones in Heterogeneous River-Aquifer Systems. Water Resources Research, 53(12): 10583–10602.

Segal E, Shouse PJ, Bradford SA, Skaggs TH, Corwin DL, 2009 Measuring Particle Size Distribution Using Laser Diffraction: Implications for Predicting Soil Hydraulic Properties. Soil science, 174(12): 639–645.

Šejna M, Šimůnek J, Genuchten M.T.v., 2018 The Hydrus Software Package for Simulating Two- and Three-Dimensional Movement of Water, Heat, and Multiple Solutes in Variably-Saturated Porous Media, User Manual, Version 3.0. PC Progress, Prague, Czech Republic, pp. pp. 322.

Šejna M, Šimůnek J, van Genuchten MT, 2014 The Hydrus Software Package for Simulating the Two- and Three-Dimensional Movement of Water, Heat, and Multiple Solutes in Variably-Saturated Porous Media, User Manual, Version 2.04.

Sidle RC, Tsuboyama Y, Noguchi S, Hosoda T, Fujieda M, Shimizu T, 2000 Stormflow Generation in Steep Forested Headwaters: A Linked Hydrogeomorphic Paradigm. Hydrological Processes, 14(3): 369–385. DOI:Doi 10.1002/(Sici)1099-1085(20000228)14:3<369::Aid-Hyp943>3.0.Co;2-P

Šimůnek J, Bradford SA, 2008 Vadose Zone Modeling: Introduction and Importance. Vadose Zone Journal, 7(2): 581–586.

Šim nek J, Šejna M, van Genuchten MT, 2007 The Hydrus Software Package for Simulating the Two- and Three-Dimensional Movement of Water, Heat, and Multiple Solutes in Variably-Saturated Porous Media, User Manual, Version 1.02, PC-Progress, Prague, Czech Republic.

Šim nek J, Šejna M, van Genuchten MT, 2018 New Features of Version 3 of the Hydrus (2d/3d) Computer Software Package. Journal of Hydrology and Hydromechanics, 66(2): 133–142. DOI: 10.1515/johh-2017-0050

Šim nek J, van Genuchten MT, Šejna M, 2016 Recent Developments and Applications of the Hydrus Computer Software Packages. Vadose Zone Journal, 15(7): 25 DOI:10.2136/vzj2016.04.0033

Sinai G, Zaslavsky D, Golany P, 1974 Influence of Anisotropy in Soil Permeability on Surface Runoff. In: Faculty of Agric. Eng. T., Haifa, Israel (Ed.).

Small EE, 2005 Climatic Controls on Diffuse Groundwater Recharge in Semiarid Environments of the Southwestern United States. Water Resources Research, 41(4).

Smith JJ, Hasiotis ST, Woody DT, Kraus MJ, 2008 Paleoclimatic Implications of Crayfish-Mediated Prismatic Structures in Paleosols of the Paleogene Willwood Formation, Bighorn Basin, Wyoming, USA. Journal of Sedimentary Research, 78(5–6): 323–334. DOI: 10.2110/jsr.2008.040

Sudicky E, MacQuarrie K, 1989 Behaviour of Biodegradable Organic Contaminants in Random Stationary Hydraulic Conductivity Fields, Kobus, HE, and Kinzelbach, W., Contaminant Transport in Groundwater, International Symposium on Contaminant Transport in Groundwater, Stuttgart, pp. 307–315.

Tseng PH, Jury WA, 1994 Comparison of Transfer Function and Deterministic Modeling of Area-Averaged Solute Transport in a Heterogeneous Field. Water Resources Research, 30(7): 2051–2063.

Turkeltaub T, Kurtzman D, Bel G, Dahan O, 2015 Examination of Groundwater Recharge with a Calibrated/Validated Flow Model of the Deep Vadose Zone. Journal of Hydrology, 522: 618–627. DOI:10.1016/j.jhydroL2015.01.026

Uchida T, Asano Y, Ohte N, Mizuyama T, 2003 Seepage Area and Rate of Bedrock Groundwater Discharge at a Granitic Unchanneled Hillslope. Water Resources Research, 39(1). DOI:Artn Artn 101810.1029/2002wr001298

USDA, 2016 Ssm - Ch. 3. Examination and Description of Soil Profiles In: Staff R.b.S.S.D. (Ed.), Soil Training. Natural Resources Conservation Service, USDA.

USEPA, 1997 Superfund Web Site. Available At: Http://Www.Epa.Gov/Superfund/Oerr/Impm/Products/Rodsites and Http://Www.Epa.Gov/Superfund/Oerr/Impm/Products/Cursites/Cercinf.Htm.

van Genuchten MT, Leij F, Yates S, 1991 The Retc Code for Quantifying the Hydraulic Functions of Unsaturated Soils. IAG-DW12933934, U.S. Salinity Laboratory, U.S. Department of Agriculture, Agricultural Research Service, Riverside, California.

Vereecken H, Kasteel R, Vanderborght J, Harter T, 2007 Upscaling Hydraulic Properties and Soil Water Flow Processes in Heterogeneous Soils. Vadose Zone Journal, 6(1): 1–28.

Vorosmarty CJ, Green P, Salisbury J, Lammers RB, 2000 Global Water Resources: Vulnerability from Climate Change and Population Growth. Science, 289(5477): 284–8. DOI:10.1126/science.289.5477.284 [PubMed: 10894773]

Wang T, Franz TE, Yue W, Szilagyi J, Zlotnik VA, You J, Chen X, Shulski MD, Young A, 2016 Feasibility Analysis of Using Inverse Modeling for Estimating Natural Groundwater Recharge from a Large-Scale Soil Moisture Monitoring Network. Journal of Hydrology, 533: 250–265.

Wang Y, Bradford SA, Šim nek J, 2014a Estimation and Upscaling of Dual-Permeability Model Parameters for the Transport of E. Coli D21g in Soils with Preferential Flow. Journal of contaminant hydrology, 159(0): 57–66. DOI:10.1016/j.jconhyd.2014.01.009 [PubMed: 24589387]

Wang Y, Bradford SA, Šim nek J, 2014b Physicochemical Factors Influencing the Preferential Transport of in Soils. Vadose Zone Journal, 13(1). DOI: 10.2136/vzj2013.07.0120

Washington State Department of Ecology, 2006 Guidance for Uic Wells That Manage Stormwater, Washington State Department of Ecology Water Quality Program.

Wilde F, 1994 Geochemistry and Factors Affecting Ground Water Quality at Three Storm Water Management Sites in Maryland, US Geological Survey, [Washington, DC.

Wood WW, Rainwater KA, Thompson DB, 1997 Quantifying Macropore Recharge: Examples from a Semi-Arid Area. Ground Water, 35(6): 1097–1106. DOI:DOI 10.1111/j.1745-6584.1997.tb00182.x

Xie Y, Cook PG, Brunner P, Irvine DJ, Simmons CT, 2014 When Can Inverted Water Tables Occur beneath Streams? Groundwater, 52(5): 769–774.

Yeh TCJ, Gelhar LW, Gutjahr AL, 1985a Stochastic-Analysis of Unsaturated Flow in Heterogeneous Soils .3. Observations and Applications. Water Resources Research, 21(4): 465–471. DOI:DOI 10.1029/WR021i004p00465

Yeh TCJ, Gelhar LW, Gutjahr AL, 1985b Stochastic Analysis of Unsaturated Flow in Heterogeneous Soils: 1. Statistically Isotropic Media. Water Resources Research, 21(4): 447–456.

Zektser IS, Lorne E, 2004 Groundwater Resources of the World: And Their Use, Ihp Series on Groundwater. UNESCO.

HIGHLIGHTS

- Recharge volume for a homogeneous domain is always smaller than for heterogeneous domains.

- Correlation between drywell infiltration and recharge volumes is highly non-linear for heterogeneous domains.

- Cumulative recharge volume increased with standard deviation and a lateral correlation length but decreased with a vertical correlation length.

- Arrival time and location increase with a lateral correlation length.

- Arrival time decreases with standard deviation and a vertical correlation length.

2D- Axisymmetric Domain
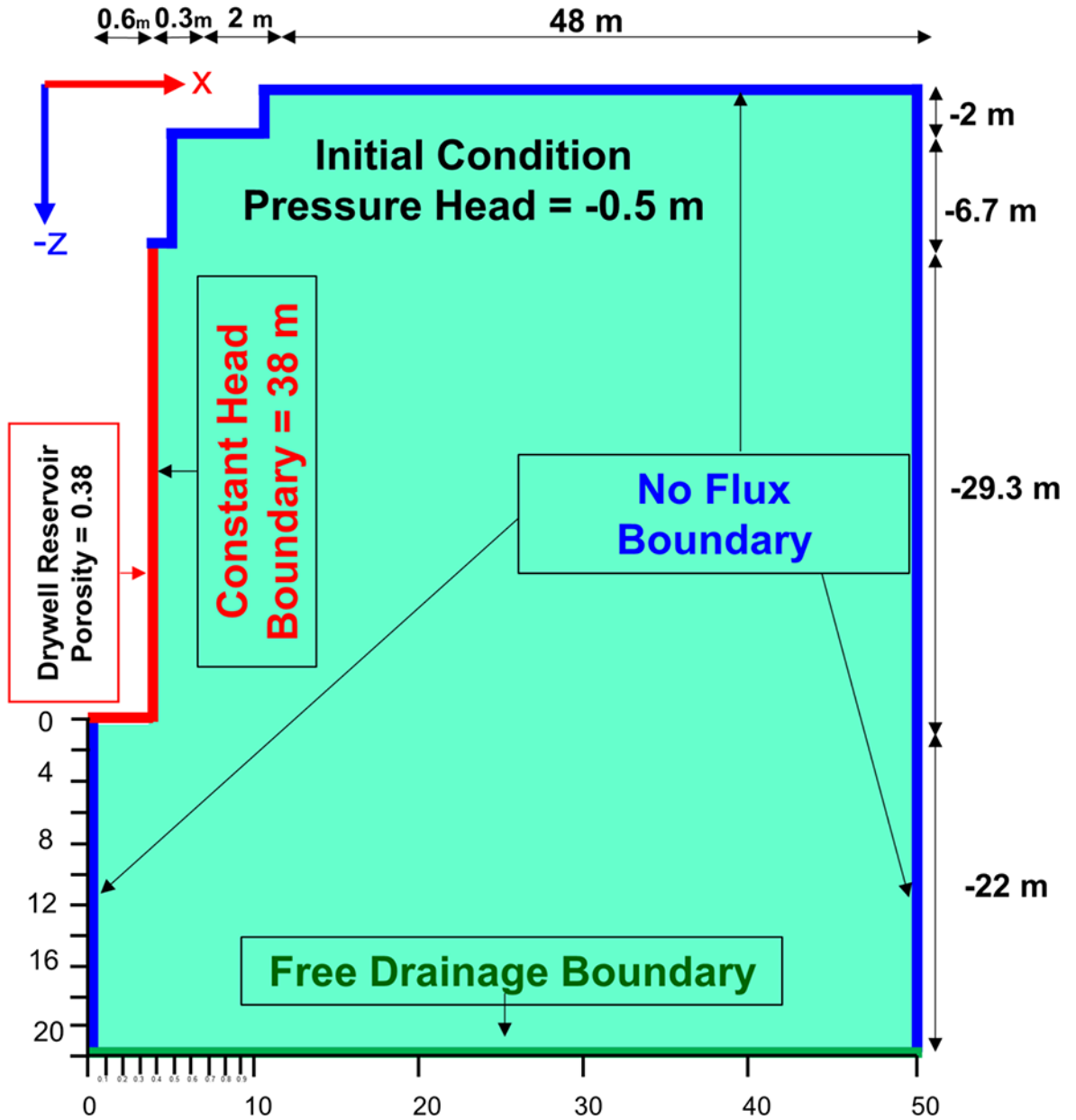
Fig. 1.
The drywell geometry, dimensions, initial condition, the boundary conditions, and X and Z correlation length scale for the 2D-axisymmetrical flow domain. The detailed drywell geometry and the water flow dynamics were presented in our previous study (Sasidharan et al., 2018a).
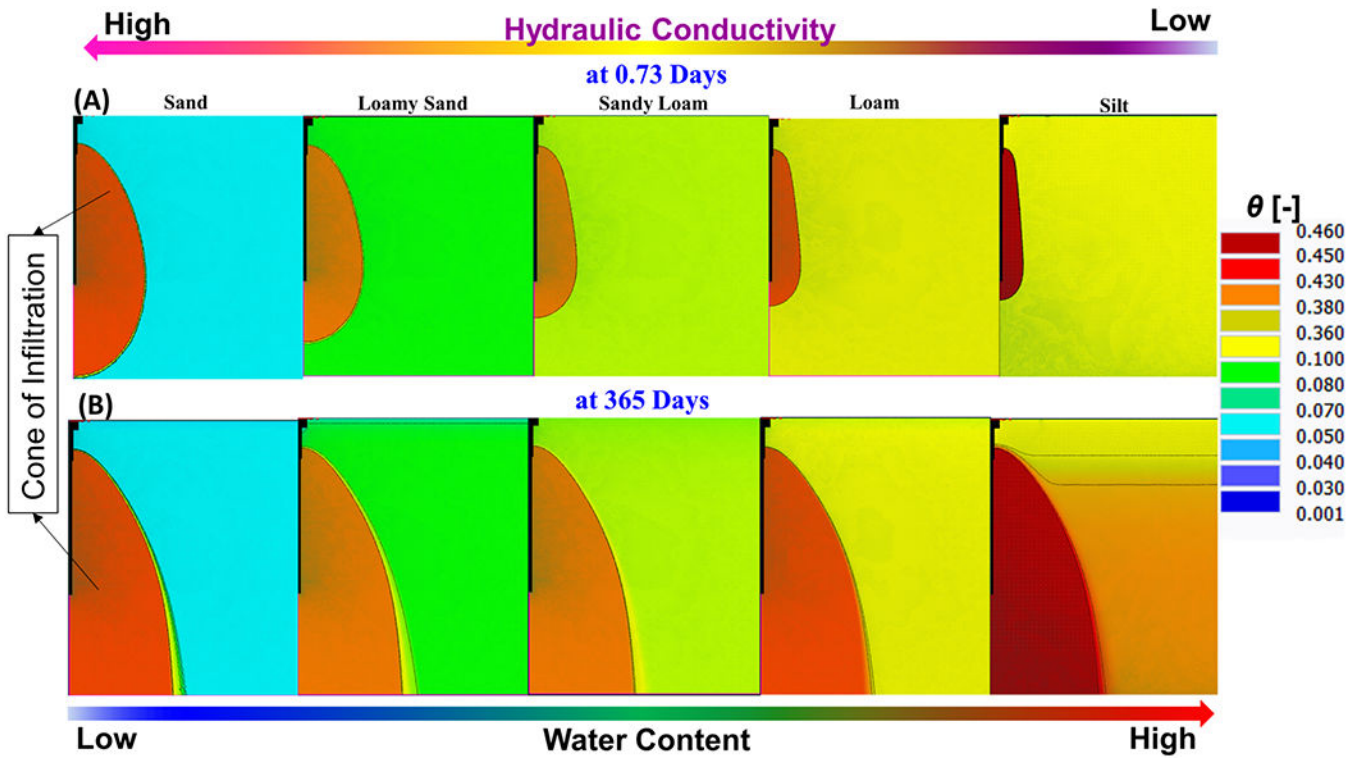
Fig. 2.
The cone of infiltration for sand, loamy sand, sandy loam, loam, and silt with hydraulic properties obtained from the HYDRUS (2D/3D) soil catalog during a constant head simulation presented as water content (θ) profiles at 0.73 **(A)** and 365 **(B)** days of simulation.
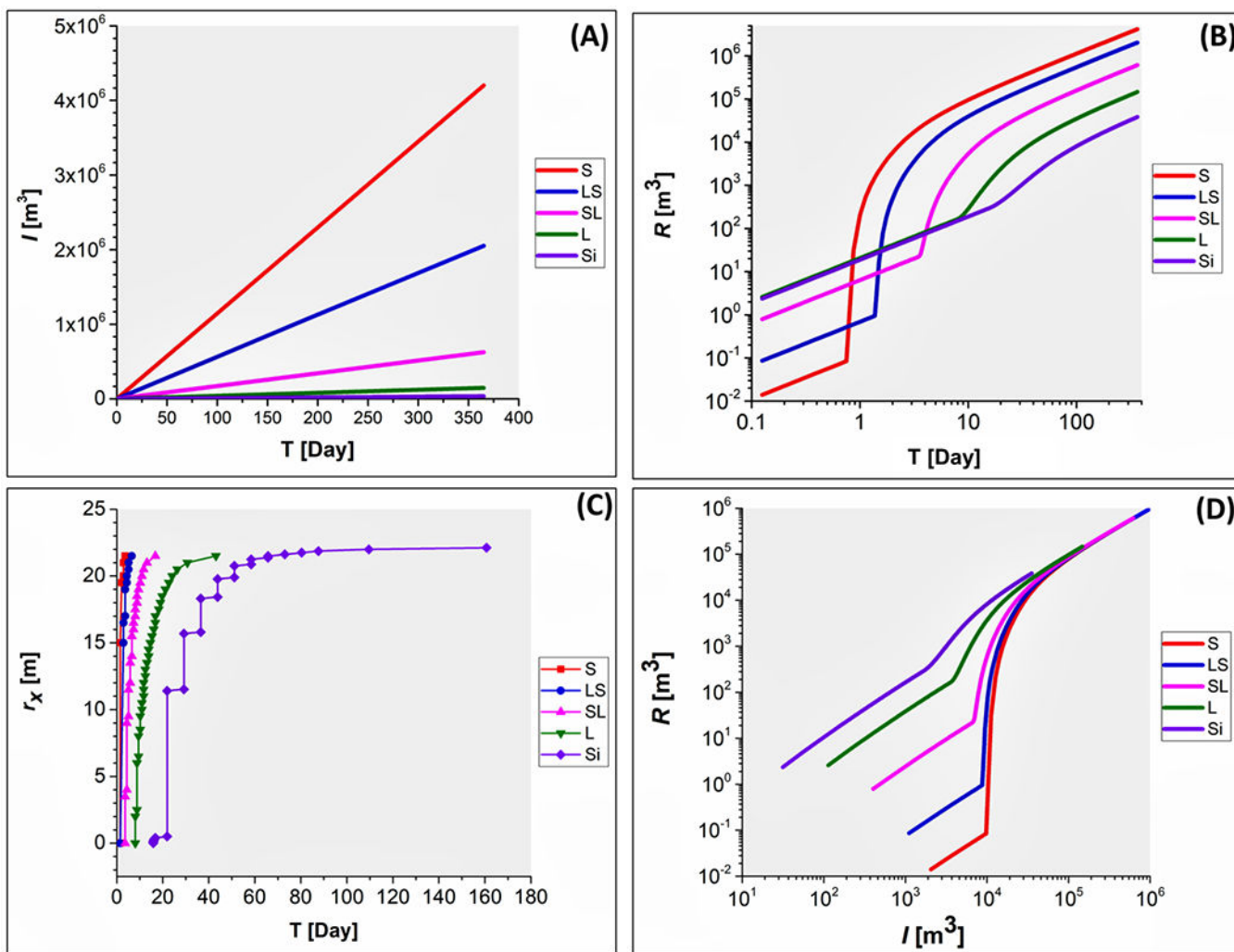
Fig. 3.
The cumulative infiltration volume (*I*) as a function of time (normal scale) (log scale is presented in Fig. S8) **(A)**, the cumulative recharge volume (*R*) as a function of time (log scale) **(B),** the radius of recharge (*r*_x) vs time of arrival at the bottom boundary **(C),** and *I* vs R (log scale) at the same time **(D)** during 365 days constant head simulation for the Sand (S), Loamy Sand (LS), Sandy Loam (SL), Loam (L), and Silt (Si) soils with hydraulic parameters obtained from the HYDRUS (2D/3D) Soil Catalog.
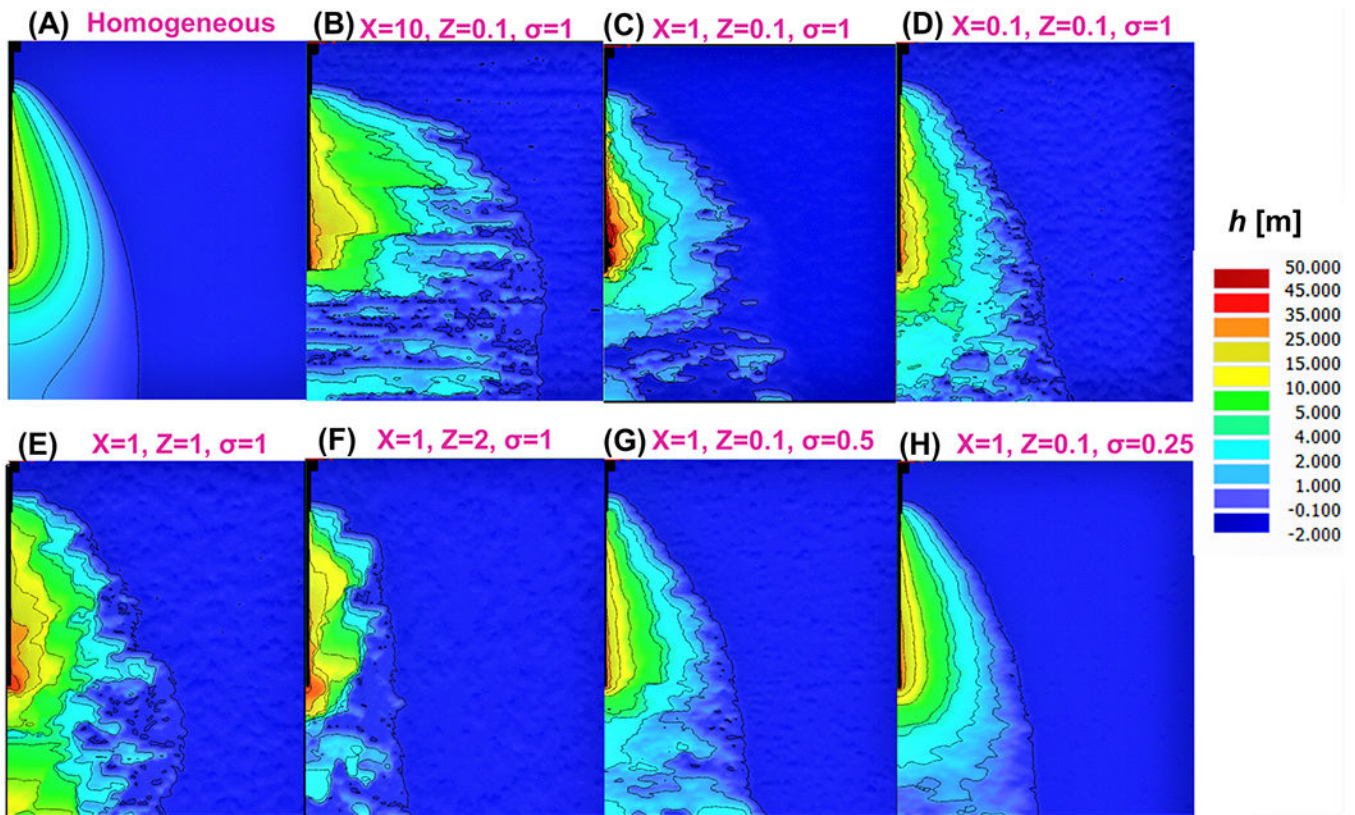
Fig. 4.
Pressure head (*h*) profiles for homogenous **(A)** and heterogeneous (*X*=10, *Z*=0.1, σ=1 (horizontal lens) **(B),** *X*=1, *Z*=0.1, σ=1 **(C),** *X*=0.1, *Z*=0.1, σ=1 **(D),** *X*=1, *Z*=1, σ=1 **(E),** *X*=1, *Z*=2, σ=1 (thick vertical lens) **(F),** *X*=1, *Z*=0.1, σ=0.5 **(G),** and *X*=1, *Z*=0.1, σ=0.25 **(H)**) Fort Irwin soil flow domains after the 1-year constant head simulation.
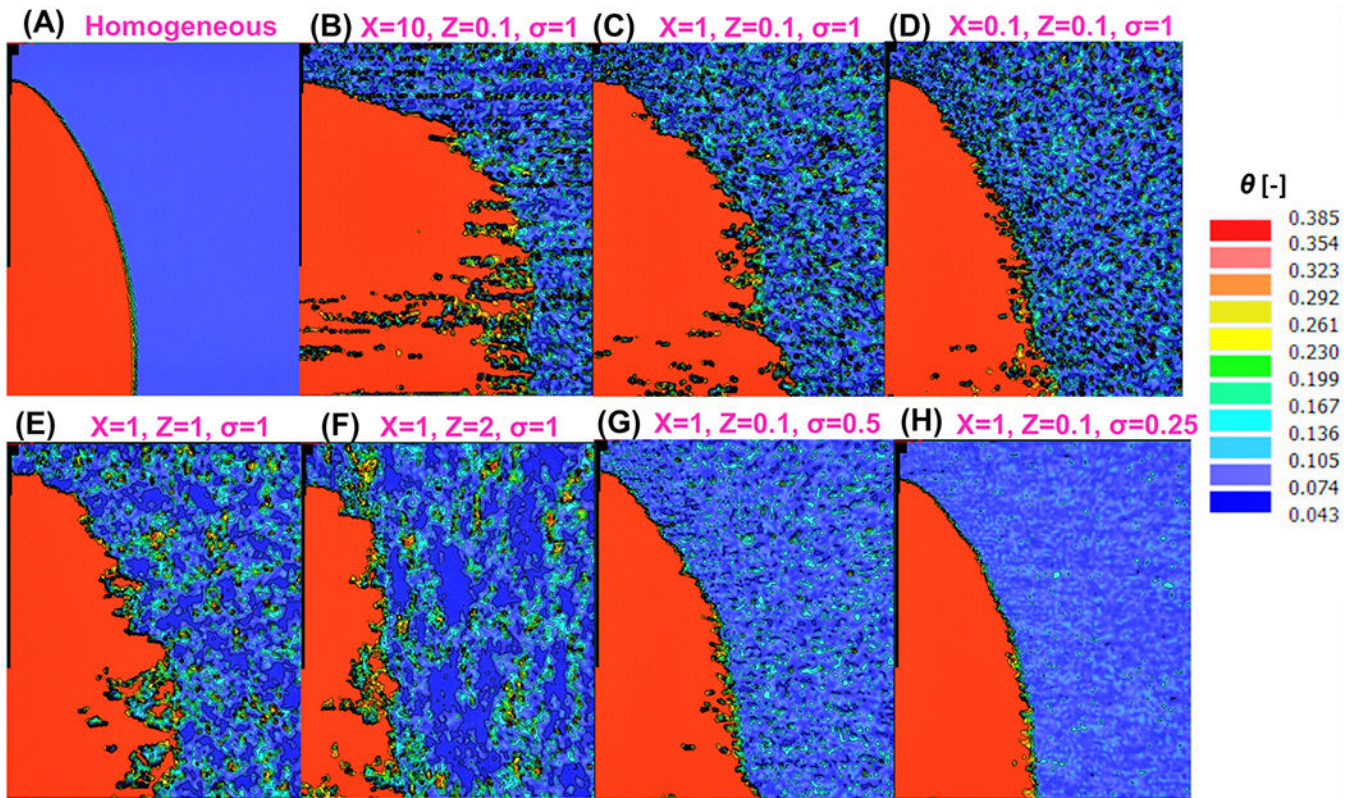
Fig. 5.

Water content (θ) profiles for homogenous **(A)** and heterogeneous (X=10, Z=0.1, σ=1 (horizontal lens) **(B),** X=1, Z=0.1, σ=1 **(C),** X=0.1, Z=0.1, σ=1 **(D),** X=1, Z=1, σ=1 **(E),** X=1, Z=2, σ=1 (thick vertical lens) **(F),** X=1, Z=0.1, σ=0.5 **(G),** and X=1, Z=0.1, σ=0.25 **(H)**)) Fort Irwin soil flow domains after the 1-year constant head simulation.
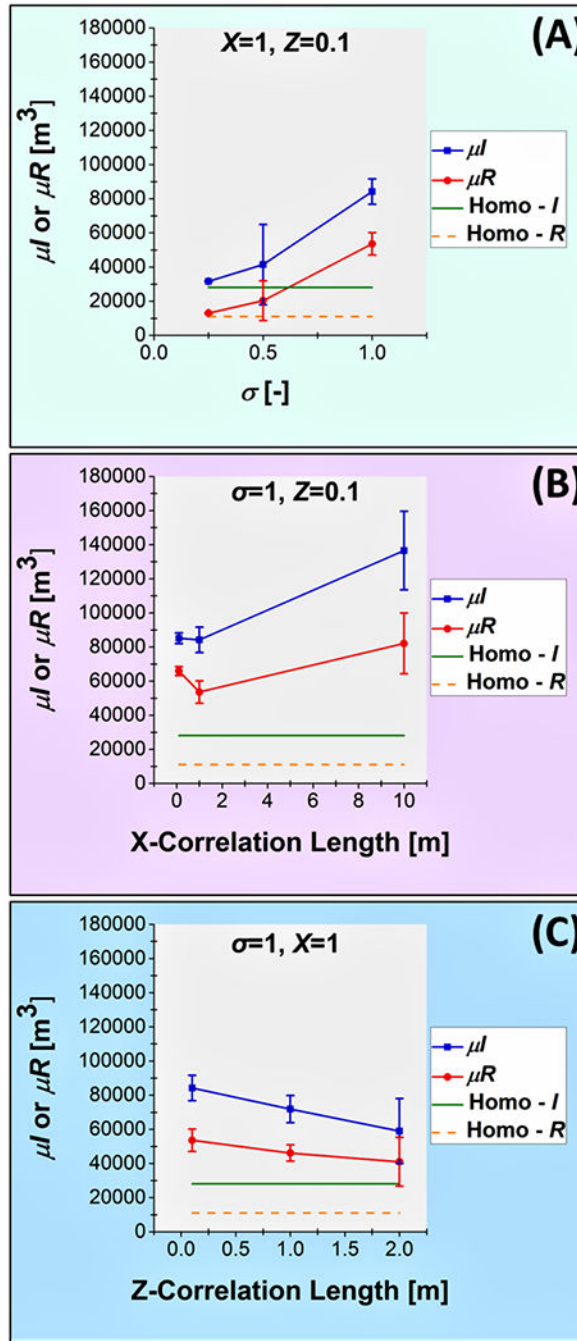
Fig. 6.
The mean cumulative infiltration volume (μI) and the mean cumulative recharge volume (μR) (from 10 simulations) and the corresponding 95% Confidence Intervals as a function of σ (σ=0.25, 0.5, 1) when X=1 and Z=0.1 **(A)**, X (X=0.1, 1, 10 m) when σ=1 and Z=0.1 **(B)**, and Z (Z=0.1, 1, 2 m) when σ=1 and X=1 **(C)** for a heterogenous Fort Irwin soil flow domain after 365 days constant head simulation. The I (Homo-I, solid green line) and R (Homo-R, dashed orange line) values after 365 days simulation for a homogeneous domain are also presented.
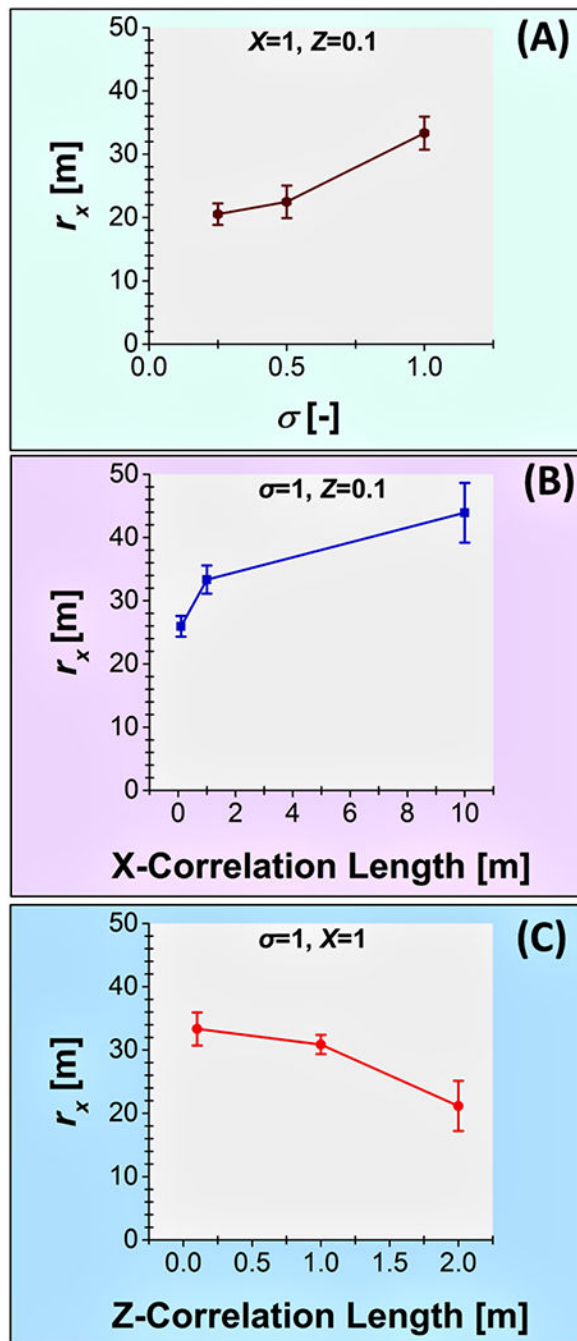
Fig. 7.
The mean radius of recharge (r_x) (from 10 simulations) and the corresponding 95% Confidence Intervals as a function of σ (σ=0.25, 0.5, 1) when X=1 and Z=0.1 **(A),** X (X=0.1, 1, 10 m) when σ=1 and Z=0.1 **(B),** and Z (Z=0.1, 1, 2 m) when σ=1 and X=1 **(C)** for a heterogeneous Fort Irwin soil flow domain after 365 days constant head simulation.
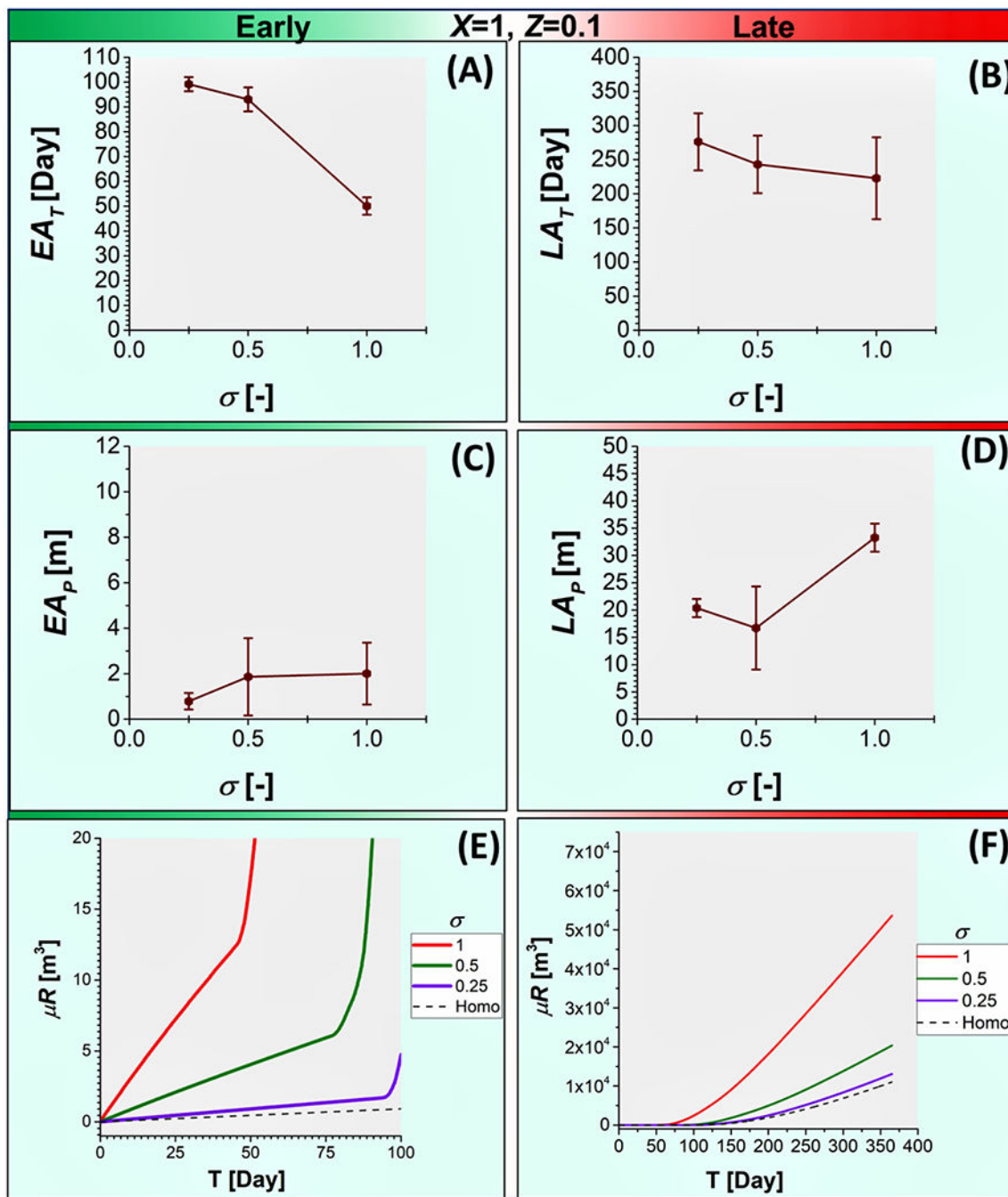
Fig. 8.
The early arrival time (EA_T) **(A),** the late arrival time (LA_T) **(B),** the early arrival point (EA_P) **(C),** the late arrival point (LA_P) **(D),** mean cumulative recharge (μR) at an early stage **(E),** and at a late stage **(F)** as a function of σ (σ=0.25, 0.5, 1) when X=1 and Z=0.1 for a heterogeneous Fort Irwin soil domain during 365 days constant head simulation.
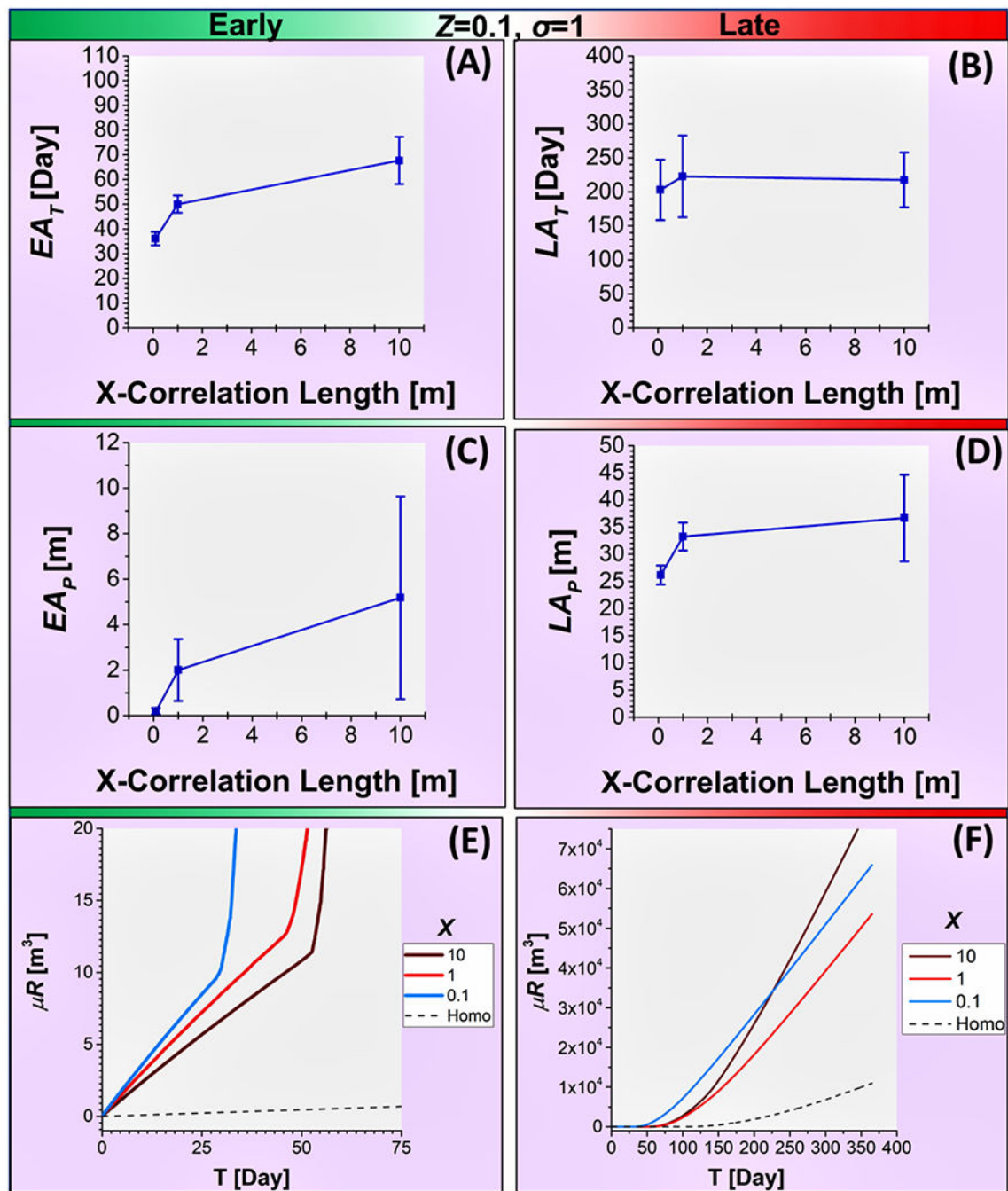
Fig. 9.
The early arrival time (EA_T) **(A)**, the late arrival time (LA_T) **(B)**, the early arrival point (EA_P) **(C)**, the late arrival point (LA_P) **(D),** mean cumulative recharge (μR) at an early stage **(E)**, and at a late stage **(F)** as a function of X (X=0.1, 1, 10 m) when Z=0.1 and σ=1 for a heterogeneous Fort Irwin soil domain during 365 days constant head simulation.
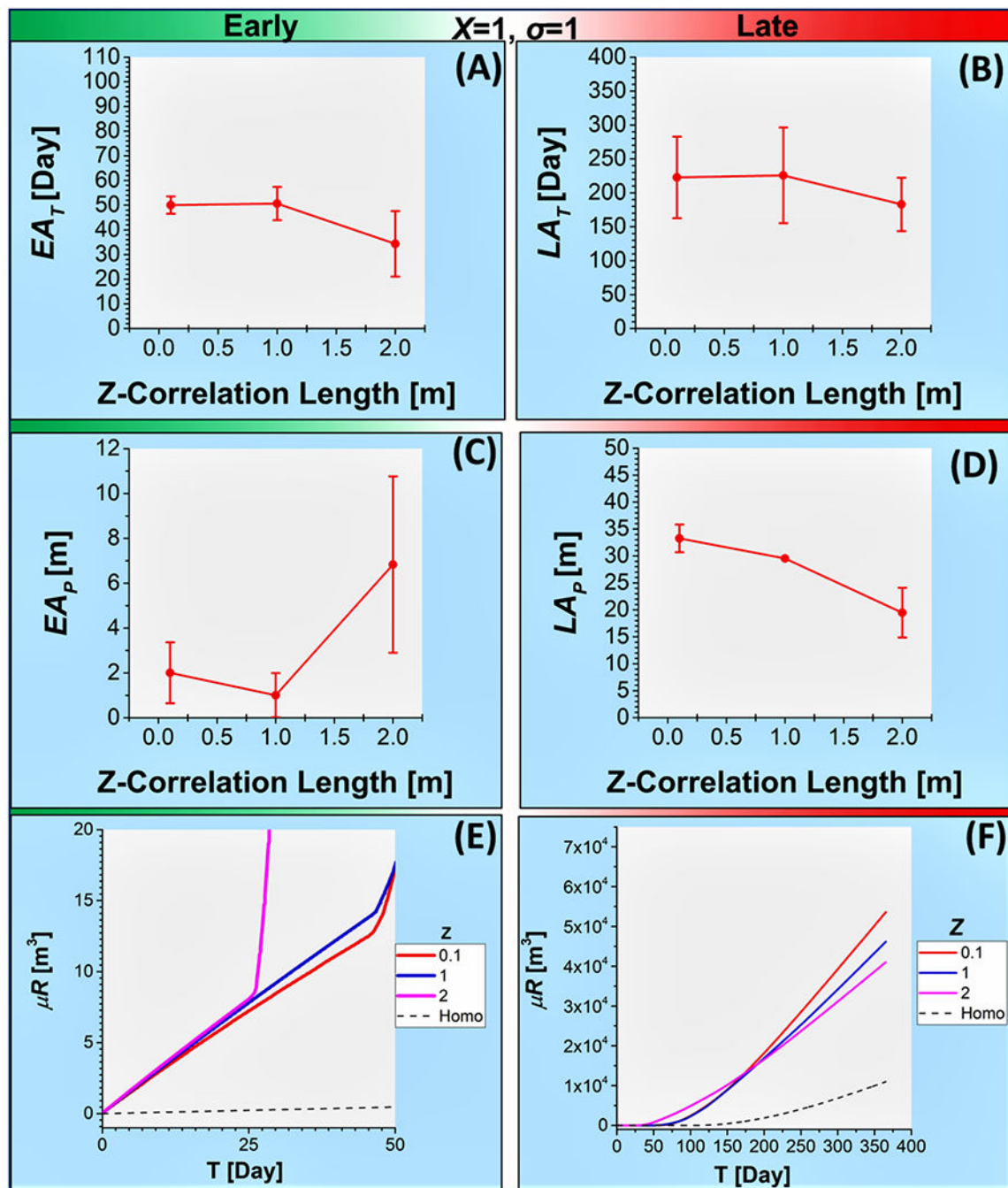
Fig. 10.
The early arrival time (EA_T) **(A)**, the late arrival time (LA_T) **(B)**, the early arrival point (EA_P) **(C)**, the late arrival point (LA_P) **(D)**, mean cumulative recharge (μR) at an early stage **(E)**, and at a late stage **(F)** as a function of Z (Z=0.1, 1, 2) when X=1 m and σ=1 for a heterogeneous Fort Irwin soil domain during 365 days constant head simulation.

Table 1.

The residual soil water content (θ_r), the saturated soil water content (θ_s), the shape parameter (α), the pore-size distribution parameter (n), the saturated isotropic hydraulic conductivity (K_s), and the tortuosity parameter (l) for different soil materials used in the numerical experiments.

Experiments	Soil	Domain	Heterogeneity	θ_r [-]	θ_s [-]	α [m⁻¹]	n [-]	K_s [m min⁻¹]	l [-]
								Soil Hydraulic Parameters	
I Soil Catalog	Sand (S) [¥]	Homogeneous	NA	0.045	0.43	14.5	2.68	4.95×10^{-3}	0.5
	Loamy Sand [LS] [¥]			0.057	0.41	12.4	2.28	2.43×10^{-3}	0.5
	Sandy Loam [SL] [¥]			0.065	0.41	7.5	1.89	7.37×10^{-4}	0.5
	Loam [L] [¥]			0.078	0.43	3.6	1.56	1.73×10^{-4}	0.5
	Silt [Si] [¥]			0.034	0.46	1.6	1.37	4.17×10^{-5}	0.5
II Stochastic Heterogeneity (Fort Irwin Soil)	Fort Irwin Soil [§]	Heterogeneous	X=10; Z=0.1; σ=1	0.043	0.39	9.17	2.76	3.20×10^{-5}	0.5
			X=1; Z=0.1; σ=1						
			X=0.1; Z=0.1; σ=1						
			X=1; Z=1; σ=1						
			X=1; Z=2; σ=1						
			X=1; Z=0.1; σ=0.5						
			X=1; Z=0.1; σ=0.25						

[¥] The values were adapted from the HYDRUS (2D/3D) Soil Catalog (Šejna et al., 2018).

[§] The value of K_S and α was obtained by the inverse optimization of the falling head experiment conducted at the Fort Irwin drywell using HYDRUS (2D/3D) as explained in our previous research (Sasidharan et al., 2018a). The values of θ_r, θ_S, and n were determined by the particle size distribution analysis using laser diffractometry device (LA930: Horiba LTD, Japan) (Segal et al., 2009) and applying the sand-silt-clay faction in the Rosetta pedotransfer function model (Schaap et al., 2001).